Chapter 5
Monitoring of the Thermal and Autogenous Strain

Brice Delsaute and Stéphanie Staquet

Abstract During early age, the autogenous and thermal deformations are two of the most important concrete properties that are involved in the cracking risk in cement-based materials and concrete structures (especially for massive structures). For that reason, several test rigs were developed in the past for the monitoring since casting time of these deformations. During early age, the thermal strain depends strongly on the evolution of the coefficient of thermal expansion (CTE), the thermal conductivity, the heat capacity, the heat release of the cement paste and the boundary conditions. During hydration process, both autogenous and thermal strains occur simultaneously and cannot be directly distinguished. In previous work, two kinds of methodology were used to monitor the CTE. The first method uses two distinct tests with two different histories of temperature in order to define autogenous and thermal strain. The second method uses only one test during which repeated thermal variations are applied to a sample. This chapter reports on the most recent advances on the physical mechanisms associated to the development of the autogenous strain and the CTE. The recent devices and test protocols developed for the simultaneous monitoring of the coefficient of thermal expansion and the autogenous strain at three different scales (cement paste, mortar and concrete) are presented. The global testing methodologies bear some similarities but major differences remain in the test set up designs, in the testing processes and also in the data processing. Based on the physical mechanisms, existing test facilities and test protocols, a new test protocol is established and is compared to existing test protocols. Finally, recommendations are proposed for the determination of the autogenous strain and the CTE.

Keywords Early age · Autogenous strain · Coefficient of thermal expansion · Heat release

B. Delsaute (✉) · S. Staquet
Service BATir, LGC, Université Libre de Bruxelles (ULB), Brussels, Belgium
e-mail: bdelsaut@ulb.ac.be

M. Serdar et al. (eds.), *Advanced Techniques for Testing of Cement-Based Materials*,
Springer Tracts in Civil Engineering, https://doi.org/10.1007/978-3-030-39738-8_5

5.1 Introduction

The free deformations are evolving quite fast during the hardening process and particularly just after the setting of the material. According to the composition, the structural and environmental situation, the amplitude of these deformations can be very significant. Dam, piers of bridge, gas containment are relevant examples for which the free deformations are important. If these deformations are partially or fully restrained, stresses are induced in the material which can lead to cracking. Therefore, it is meaningful to consider correctly the development of the free deformation in the design of concrete structures which are massive, use low water-cement ratio or silica fume, or which need to be waterproof or airtight. When the material is not exposed to drying, the free deformations of the material after setting are composed by the autogenous deformation ε_{au} and the thermal deformation $\varepsilon_{\mathrm{th}}$:

$$\varepsilon_{\mathrm{f}}(\mathrm{t}) = \varepsilon_{au}(\mathrm{t}) + \varepsilon_{\mathrm{th}}(\mathrm{t}) = \varepsilon_{\mathrm{au}}(\mathrm{t}) + \int_0^{\mathrm{t}} \alpha_{\mathrm{T}}(\mathrm{t}) \cdot \dot{\mathrm{T}} \cdot \mathrm{dt} \tag{5.1}$$

The thermal deformations are function of the evolution of the temperature inside the concrete material and the evolution of the coefficient of thermal expansion α_{T} (CTE, expressed in $°\mathrm{C}^{-1}$) of the concrete (Eq. 5.1). The evolution of the temperature depends on the boundary conditions and the dimensions of the structure and the evolution of materials properties of the concrete. The evolution of the temperature caused by the hydration of cement is defined by solving the heat equation (Eq. 5.2) for which the density ρ (expressed in kg m^{-3}), the thermal conductivity λ (expressed in W m^{-1} K^{-1}), the heat capacity $\mathrm{C_p}$ (expressed in J $°\mathrm{C}^{-1}$), and the heat release by the concrete during hydration process Q (expressed in J g^{-1}) must be known.

$$\rho \cdot \mathrm{C_p} \cdot \frac{\partial \mathrm{T}}{\partial \mathrm{t}} = \mathrm{div}(\lambda \cdot \mathrm{gradT}) + \frac{\partial \mathrm{Q}}{\partial \mathrm{t}}. \tag{5.2}$$

The heat release, the thermal conductivity, the heat capacity and the density are material parameters which evolve during the hydration process and are necessary to know in order to define the evolution of the temperature. The heat release can be determined by using adiabatic calorimetry (Darquennes 2009), semi-adiabatic calorimetry (Boulay et al. 2010) or isothermal calorimetry (Instruments 2017). The thermal conductivity and the heat capacity can be determined by generating a thermal gradient inside the sample and measuring the temperature distribution (Campbell-Allen and Thorne 1963; Mounanga et al. 2004; Bentz 2007). The coefficient of thermal expansion can be determined by applying thermal variations on a specimen. Nevertheless, the monitoring of the CTE and the autogenous deformation remains difficult to assess during early age. As a matter of fact, during the hardening process both parameters evolve at the same time. Displacements due to both are superimposed during the measurement.

In the present chapter, a new test protocol is developed for the monitoring of the autogenous strain and the coefficient of thermal expansion since setting. First, an initial overview of the physical mechanisms related to the development of the autogenous strain and the coefficient of thermal expansion is presented. The recent devices developed and their associated test protocol for the characterization of both properties at the three scales (cement paste, mortar and concrete) are then presented and compared. Based on the physical mechanisms, existing test facilities and test protocols, a new test protocol is established. The results obtained on an ordinary concrete with the BTJADE (Boulay 2012) device are presented then. A sensitivity analysis is performed in order to highlight the importance of the data processing in the determination of the CTE. Finally, an extension of this methodology on cement paste and mortar is presented and recommendations are proposed for the determination of the autogenous strain and the CTE.

5.2 Physical Mechanisms

5.2.1 Autogenous Deformation

Le Chatelier (1900) has first shown that the hydration of cement causes shrinkage, because the volume of hydration products is lower than the volume of reactants. This is known as chemical shrinkage. As long as cement paste remains fluid, autogenous deformation is equal to chemical shrinkage (Fig. 5.1a). When the material sets, the stiffness of the skeleton of the cement paste increases and a restriction of the chemical shrinkage takes places (Bouasker et al. 2008). Then, chemical shrinkage is not transformed in volumetric strain due to the formation of a gaseous volume phase in the pore (because of the water consumption by the hydration reaction). The internal voids, or capillarity pores, created in the cement paste cause self-desiccation shrinkage (Fig. 5.1b). Capillarity pores have a size ranging from 10 nm to 10 μm

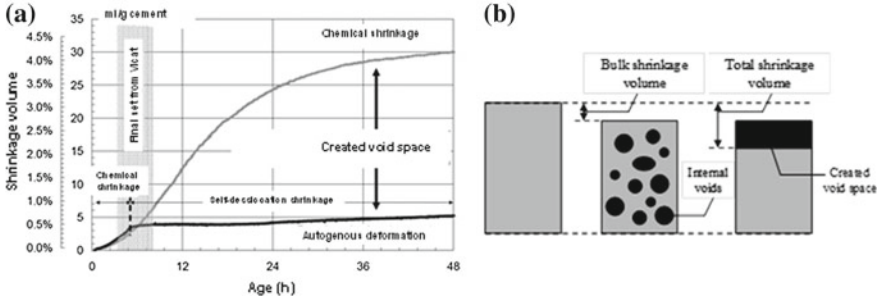

Fig. 5.1 **a** Chemical shrinkage and autogenous deformation (Bouasker 2007), **b** definition of autogenous shrinkage after setting (Garcia Boivin 1999)

(Mindess et al. 2003). Most of studies dealing with autogenous deformation actually refer to self-desiccation, in other words autogenous shrinkage after setting. However, at the very early stages after setting, some cementitious materials exhibit swelling during several hours or days before shrinking (Darquennes et al. 2011; Delsaute and Staquet 2017a).

Despite the many studies carried out in the paste, there is still no general consensus on the mechanisms related to the swelling. Three reasons were observed:

1. **The water absorption of cement paste during hydration** due to bleeding or due to the internal curing coming from porous aggregate (e.g. lightweight aggregate (Kohno et al. 1999; Liu and Hansen 2016) and recycled aggregate (Delsaute and Staquet 2017b, 2019), fillers (Esping 2008; Craeye et al. 2010) or super absorbent polymer (Wyrzykowski and Lura 2013a) which cancels the self-desiccation phenomenon.
2. **The volume of the hydration product**, swelling is also linked to the formation and growth of portlandite crystals (Baroghel-Bouny et al. 2006; Sant et al. 2011; Stefan et al. 2018) and ettringite (Mehta 1973). The formation of both elements will lead to a crystallization stress. These stresses depend on many factors such as the size of the elements and their growth direction (Min and Mingshu 1994; Odler and Colán-Subauste 1999), porosity (size distribution and quantity), the E-modulus and the creep of the cement paste (Chaunsali and Mondal 2016).
3. Another source of swelling comes from **measurement artifacts**. The removal of the thermal strain needs an accurate knowledge of the evolution of the coefficient of thermal expansion during the whole hydration process which is generally not the case (Bjøntegaard et al. 2004). Secondly, round-robin testing (Bjøntegaard et al. 2004) have shown quite important dispersion between results from different laboratory and different test rigs (Bjøntegaard et al. 2004).

The autogenous shrinkage is related to the self-desiccation of the cement paste during the hydration process. This results in a decrease of the relative humidity till a value of around 75% (Le Roy 1995; Barcelo et al. 1999; Hammer 2003; Eppers and Mueller 2008). In this range, the mechanisms involved in self-desiccation shrinkage are capillary tension, disjoining pressure and surface tension (Brooks and Megat Johari 2001).

Capillary pores are initially filled with water. As water is consumed by the hydration of cement, voids appear and liquid-vapour menisci are created in the pores. Thus capillary tension develops in the pore water and compressive stresses are generated in the solid. By considering Young-Laplace and Kelvin laws, the capillary depression σ_{cap} can be expressed as a function of the radius of capillary pores or the internal relative humidity:

$$\sigma_{cap} = P_g - P_l = \frac{R \cdot T \cdot \rho_e}{M} \cdot \ln(RH) = \frac{2 \cdot \sigma}{r} \cdot \cos \alpha_m \tag{5.3}$$

where P_g is the pressure in gaseous phase (air + vapour) [Pa], P_l is the pressure in liquid phase (water) [Pa], R is the universal gas constant [8.314 J mol^{-1} K^{-1}],

T is the temperature [K], ρ_e is the density of water [kg m^{-3}], M is the molar mass of water [kg mol^{-1}], RH is the internal relative humidity, defined as the ratio of vapour pressure to saturated vapour pressure, σ is the surface tension of pore fluid ($\sigma = 72.75 \times 10^{-3}$ N m^{-1} for water) [N m^{-1}], r is the radius of curvature of the meniscus of the pore size [m], and α_m is the liquid-solid contact angle [rad]. From the latter equation, it follows that the finer the capillary pores, the higher the capillary depression, and that large capillarity pores dry first. The hydration products progressively fill the porosity of cement paste and refine the capillary porosity, thus the hydration reactions cause changes in moisture capacity (adsorption isotherm) of cement paste (Xi et al. 1994). The internal surface of hydration products increases which induces a redistribution of pores water and a growing effect of surface forces of solid gel particles. As a consequence effective pore pressure and self-desiccation shrinkage increases as hydration goes on (Bentz et al. 1998; Coussy 2003).

Disjoining pressure develops in the microstructure of cement paste in the areas of hindered adsorption. The formulation of this approach of hindered adsorption was first developed by Powers (1968), then by Feldman and Sereda (1968), Bažant (1972) and Ferraris and Wittmann (1987), Beltzung and Wittmann (2005). At a given temperature, the thickness of the adsorbed water layer depends on the local relative humidity. If the distance between two solid surfaces is lower than two times the thickness of the free adsorbed layer, adsorption is hindered and disjoining pressure develops. It tends to separate the adjacent surfaces. A decrease of the relative humidity results in a reduction of this pressure and causes shrinkage.

The surface tension concerns materials with a large internal surface, such as hydrating cement pastes and cement-based materials (Wittmann 1968). According to Bangham and Fakhoury (1931), a local increase in relative humidity of dry material results in a reduction of surface tension and an expansion. The adsorbed water actually reduces surface tension and lowers the hydrostatic pressure of the gel particles. Therefore, when the thickness of water adsorbed on solid surface is reduced, as it is the case during the hydration process, an increase of the surface tension of the solid occurs and leads to shrinkage. However, the changes of surface tension play a role minor in case of high relative humidity (Powers 1965) as it is the case in sealed condition for cement based materials (Le Roy 1995; Barcelo et al. 1999; Hammer 2003; Eppers and Mueller 2008).

As the interactions between hydration products and the pore solution are not fully understood, research is still needed to understand the mechanisms related to autogenous shrinkage and swelling.

Autogenous shrinkage is influenced by the main composition parameters of concrete, namely: W/C-ratio (Delsaute and Staquet 2017a), cement or binder type (Benboudjema et al. 2019; Staquet et al. 2019), volume of paste and aggregate (Liu and Hansen 2016) and nature of aggregate [porosity (Maruyama and Teramoto 2012) and stiffness (Le Roy 1995)].

5.2.2 Coefficient of Thermal Expansion

The coefficient of thermal expansion (CTE) expresses the variation in a unit length of a material in response to a change in temperature. The CTE is indicated as a linear change (linear expansion coefficient α_T in µm/m/°C) or as a volumetric change (volumetric expansion coefficient β_T in $\mu m^3/m^3/°C$). The volumetric CTE can be approximated as 3 times the linear one. In cement based materials, the coefficient of thermal expansion depends mainly on the internal relative humidity of the cement paste and the nature of the aggregate (fib 2013; Siddiqui and Fowler 2014, 2015). During the hardening process, 4 stages occur (Sellevold and Bjøntegaard 2006) as shown in Fig. 5.2. First the value of the CTE is very high due to the contribution of water when the cement paste is still in a plastic phase. When the cement paste starts to set, a sudden decrease of the CTE is observed till a minimum value corresponding to the CTE of the solid skeleton. During this second stage, the evolution of the CTE is driven by the amount of water which is no yet chemically bound and by the increase of the stiffness of the cement paste. Then an increase of the CTE is observed and is due to the decrease of the internal relative humidity in the cement paste. Finally, no significant evolution of the CTE is observed after a certain age even if the material is still hydrating. This age is function of the composition of the material and the curing temperature. During this last stage, only the boundary conditions and the associated environmental conditions (external relative humidity) of the concrete structure affect the magnitude of the CTE. Therefore the CTE has a minimum value around the setting time. For compositions with low water-cement ratio, a factor 2 can be observed between this minimum and the value of the CTE obtained after several weeks (Sellevold and Bjøntegaard 2006).

During the third and fourth stage, the CTE varies according to the change in the internal relative humidity of the cement paste induced by the hydration process and/or the environmental conditions. Two contributions have to be considered to define the magnitude of the CTE: the thermal expansion of the solid body, which is caused by the molecular movement of the cement paste, and the hygro-thermal mechanism (Bažant 1970; Wyrzykowski and Lura 2013b). Sellevold and Bjøntegaard (2006) have shown that the thermal dilation of the solid body is nearly independent of the

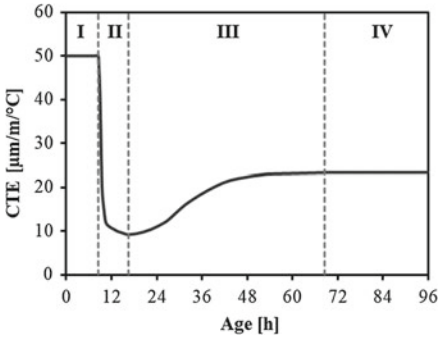

Fig. 5.2 Typical evolution of the CTE of a cement paste

saturation state of the cement paste and that hydration has a very low effect on the dilation of the solid skeleton. In addition, this dilation takes place immediately when the temperature of the solid skeleton changes.

As already mentioned, the magnitude of the CTE is strongly related to the moisture content of the cement paste and, in particular, to the change of internal relative humidity (Grasley and Lange 2006; Sellevold and Bjøntegaard 2006; Yeon et al. 2009; Wyrzykowski and Lura 2013b). A decrease of the internal relative humidity causes an increase of the CTE. The internal relative humidity is function of the temperature. Thus, in a cement based material, an increase of the temperature leads to an increase of the internal relative humidity (Jensen and Hansen 1999) and therefore to a decrease of the CTE. The hygrometric coefficient $\Delta RH/\Delta T$ is used to quantify the change of RH as a result of the unit change of temperature. In Fig. 5.3, based on several results coming from the literature (Bažant 1970; Nilsson 1987; Persson 2002; Radjy et al. 2003; Grasley and Lange 2006), a typical evolution of the hygrometric coefficient is shown as a function of the internal relative humidity of a cement paste. An asymmetrical bell-shaped is observed between both parameters. A maximum is reached around a relative humidity of 60%. Whatever the relative humidity, the hygrometric coefficient is always positive. Between a range of relative humidity between 50 and 100%, the hygrometric coefficient increases when the relative humidity decreases. For relative humidity lower than 50%, a decrease of the hygrometric coefficient is observed. In case of early age concrete in sealed condition, the internal relative humidity of the cement paste is higher than 75% (Le Roy 1995; Barcelo et al. 1999; Hammer 2003; Eppers and Mueller 2008). In such range of relative humidity, the hygrometric coefficient increases always when the relative humidity decreases. This explains why the CTE increases during the hardening process with the self-desiccation of the cement paste. This evolution of the hygrometric coefficient is associated to the redistribution of liquid water inside the cement paste. According to Bazant (1970), water migrates from gel pores to capillary pores when the temperature increases. Recently Wang et al. (2018) have shown

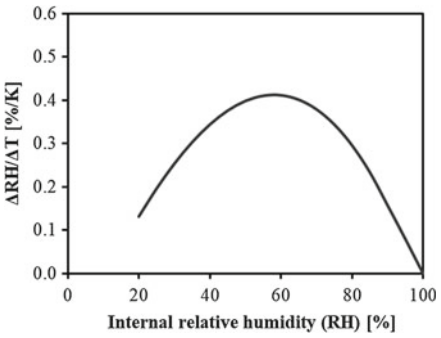

Fig. 5.3 General scheme of evolution of the hygrothermic coefficient of cement paste as a function of the internal relative humidity based on results from the literature (Bažant 1970; Nilsson 1987; Persson 2002; Radjy et al. 2003; Grasley and Lange 2006)

by using micro-poromechanics with a three-scale representation of the cement paste that the hydrometric coefficient is related to the quasi-instantaneous transfer of water between the hydrates and the nanoscopic pores and to the change in pore pressure associated to this water transfer.

Several authors (Bažant 1970; Day 1974; Wittmann and Lukas 1974) reported that the CTE is composed of an **instantaneous and delayed terms**. It was observed that the delayed term is function of the temperature history and the internal relative humidity. The thermal strain induced by the pure thermal dilation of the solid skeleton and the change of internal relative humidity caused by temperature changes develops very fast and consequently are considered to be nearly instantaneous. According to Wyrzykowski and Lura (2013a, b), these thermal strains refer to a time spans ranging from minutes to hours. This time is needed to reach thermal equilibrium and quasi-equilibrium of the corresponding thermal strain in the sample. These mechanisms are responsible of water redistribution between gel and capillarity pores causing delayed thermal shrinkage/swelling. The delayed deformations are also induced by the pressure dissipation in pores which causes a delayed recovery of pure thermal dilation (Scherer 2000, 2003).

Aggregates are inert and have a diluting effect on the evolution of the CTE. After setting, the CTE of a cement paste ranges from 8 to 25 μm/m/°C while the CTE of aggregate is generally smaller with a magnitude ranging from 4 to 14 μm/m/°C according to its mineral composition (Johnson and Parsons 1944). Consequently, for concrete material, an incompatibility of the free thermal strain of the component exists and leads to an internal restraint of the displacement of the cement paste resulting in stress development which may cause micro-cracking and reduce the durability of concrete elements (Cagnon et al. 2016).

The coefficient of thermal expansion is influenced by the main composition parameters of concrete, namely: the nature, the porosity and the content of gravels (Kumar Mehta and Monteiro 2006; Maruyama and Teramoto 2012; Delsaute and Staquet 2017b), the type, the fineness and content of the cement, including type and amount of supplementary cementitious materials (Mitchell 1953; Emanuel and Hulsey 1977; Maruyama et al. 2014; Delsaute and Staquet 2017a), and the adding of other admixture such as super absorbent polymer (Wyrzykowski and Lura 2013a; Staquet et al. 2019). The sand-aggregate ratio, the nature of the sand and the temperature do not affect significantly the magnitude of the CTE of concrete (Ziegeldorf et al. 1978; Alungbe et al. 1992; Maruyama et al. 2014). The water-to-cement ratio changes the evolution of the CTE during the hardening process but does not change significantly the amplitude of the CTE of hardened cement paste (Maruyama et al. 2014) and concrete (Delsaute and Staquet 2017a).

5.2.3 *Correlation Between the Development of the Autogenous Strain and the CTE*

Delsaute and Staquet (2017a) have compared the evolution of the autogenous strain and the CTE for concrete compositions with a water-to-binder ratio of 0.4, 0.5 and 0.6. It was observed that the evolution of both parameters is linked. For each composition, the CTE and the autogenous strain evolve in an opposite direction during the whole test duration and the maximum of the autogenous swelling takes place when the CTE reaches a minimal value. In other words, when concrete exhibits swelling, the CTE decreases while shrinkage is observed when the CTE increases. In addition, results of the CTE were plotted in function of the autogenous strain (Fig. 5.4 for the swelling period and Fig. 5.5 for the shrinkage period). For this comparison, autogenous strain was set to zero when the maximum of swelling is reached. For each composition, a linear relation was observed and is function of the water-to-cement ratio and the nature of the binder during early age. It was therefore concluded that the mechanism related to the expansion of the concrete is also linked to the decrease of the CTE. The increase of the CTE and the autogenous shrinkage are correlated to the mechanism of self-desiccation of the cement paste as explained in previous sections. These observations were then confirmed on mortar with different type of

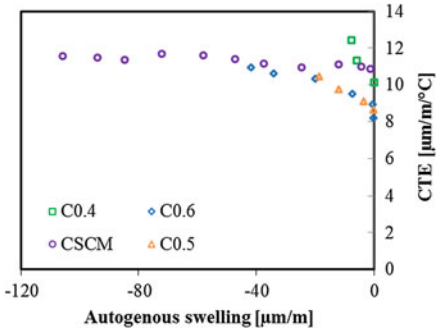

Fig. 5.4 Evolution of the CTE according to the autogenous swelling (Delsaute and Staquet 2017a)

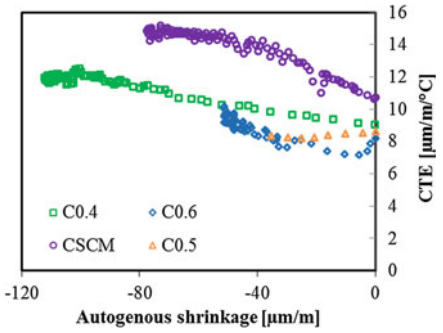

Fig. 5.5 Evolution of the CTE according to the autogenous shrinkage (Delsaute and Staquet 2017a)

cement (Milenkovic et al., no date) and concrete composed of recycled aggregate (Delsaute and Staquet 2017b, 2018a, b, 2020).

5.3 Test Setup

The characterization of the autogenous strain is very sensitive to the conditions of storage of the specimen and to many factors related to the test rig. For that reason several recommendations were developed in the past (Jensen and Hansen 2001; Hammer and Bjøntegaard 2006; ASTM Standard C1698 2014; Bjøntegaard et al. 2015). The main common requirements for all the apparatus for autogenous deformation test are their ability to:

– perfectly seal the specimen in order to avoid any external drying or water uptake;
– keep the temperature constant, which requires external control because the hydration of cement paste releases heat;
– limit the friction with the specimen.

Several devices aimed at monitoring the autogenous deformations were developed in the past. The methods can be in general divided in two categories: linear (Paillere and Serrano 1976; Baroghel-bouny 1994; Kovler 1994; Kronlöf et al. 1995; Mejlhede Jensen and Freiesleben Hansen 1995; Bjontegaard 1999; Bouasker 2007; Boulay 2012) and volumetric (Loukili et al. 2000; Charron 2003; Mitani 2003; Bouasker 2007; Stefan 2009; Loser et al. 2010; Wyrzykowski and Lura 2013a, b). Whereas volumetric methods are mainly used on cement pastes and mortars, the linear methods have been used on three scales including concrete. Horizontal and vertical setups have been designed. Both methods can be divided into two groups: rigid moulds and flexible moulds. Rigid moulds have been reported to underestimate the magnitude of autogenous shrinkage because of friction between the specimen and the mould. It is assumed that volumetric free deformations are isotropic. Thus volumetric free deformation corresponds to three times of the linear one. Zhutovsky and Kovler (2017) have shown that results obtained with both methods are close when considering the maturity of the samples. However, no clear evidence of this relation has been shown in the literature till now. This could be explained by the different artifacts of measurement coming from volumetric and linear methods. In the linear method, elongation and shortening of the sample is monitored with either direct measurement of the sample length change or by displacement measurement with e.g. LVDT, strain gauges (Boulay 2003). For correct consideration of the temperature variation, it is needed to have knowledge in depth of the thermal sensitivity of the test rig. The volume change of the cement paste or mortar is monitored by using hydrostatic weighing method. The sample is immersed in a bath containing liquid of known density and is supported to a scale. The volume change is measured through the apparent mass changes of the immersed sample. This method was significantly improved during the last decade in order to remove artifacts coming from the absorption of the water by the membrane (Mitani 2003), the liquid used for the

thermal regulation (Lura and Durand 2006), bleeding of the cement paste (Le Roy 1995).

No standard was developed till now for the simultaneous monitoring of the autogenous strain and the coefficient of thermal expansion since setting. However, as mentioned in (Benboudjema et al. 2019), the ASTM C1698-09 (ASTM Standard C1698 2014) standard exists for the determination of the autogenous strain since setting on cement paste and mortar. No standard has been developed for concrete. For the CTE, the ASTM C531-00 (ASTM C531-00 2012) standard was developed for hardened mortar and concrete. Hammer and Bjøntegaard (2006) have developed a recommendation for the simultaneous characterization of the autogenous strain and the CTE. In addition to the requirements stated above, the test rig should be designed with the consideration of several other performance criteria:

- the side, length or diameter of the sample must be 4 times higher than the nominal maximum diameter of the aggregate;
- Thermal gradient between the core and the surface of the specimen and between the core of the specimen and the target temperature must be never more than 2 °C;
- Thermal dilation of the test rig and/or the measuring devices must be minimized and controlled. This means that the test rig and/or measuring devices must be calibrated;
- During the first 24 h after the final setting of the material, measuring intervals must be less than 15 min. Measurements must continue till an age of 2 weeks minimum;
- The resolution of the measurement devices must be less than 15 μm/m;
- In case of bleeding, arrangement must be taken in order to minimize its effect. Rotation of the specimen or removal of the bleed water on the top surface of the specimen at the end of the bleeding period can prevent effect of bleeding on the development of the autogenous strain and the CTE.

5.3.1 Cement Paste and Mortar

Volumetric and linear methods were developed for the monitoring of the autogenous strain and the coefficient of thermal expansion on cement paste and mortar. Loser, et al. (2010) have developed a volumetric method for which a sample with a mass of around 20–30 g is inserted in an elastic membrane. The sample is hung to a high accuracy scale (sensitivity of 0.1 mg and accuracy of 0.28 mg), then immerged in an oil bath and placed in a permeable box which reduces strongly the impact of oil circulation induced by the thermal regulation on the weight measurement. The temperature around the sample is measured and is considered as the temperature of the cement paste or mortar during the test for the determination of the autogenous strain and the coefficient of thermal expansion. In order to validate the test rig, results of the autogenous strain and the coefficient of thermal expansion were compared to results obtained on prisms (linear method) and a good agreement was observed. The test rig is shown in Fig. 5.6.

Fig. 5.6 Volumetric testing device designed for cement paste and mortar with a sample weight of 25–30 g (Loser et al. 2010)

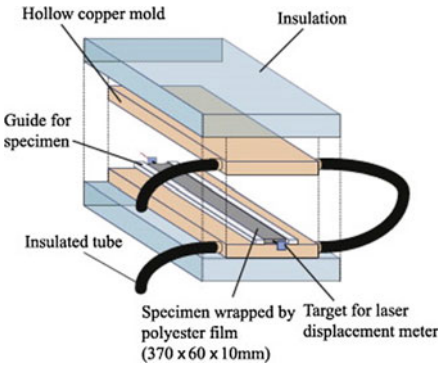

Fig. 5.7 Linear horizontal testing device designed for cement paste and mortar with laser displacement sensor in a 370 × 60 × 10 mm beam (Maruyama and Teramoto 2012)

Maruyama and Teramoto (2011) have developed a horizontal device for which the sample has a cross section of 10 mm × 60 mm and a length of 370 mm (Fig. 5.7). The sample is casted in a hollow copper mold in which water from temperature controlled water tank circulates. A layer of polyester with a thickness of 0.05 mm is placed between the sample and the mold in order to reduce the friction and to keep the material in sealed condition. The whole system is surrounded by an insulation to improve the efficiency of the thermal regulation. The temperature of the sample is recorded with two thermocouples placed in one extremity and in the center of the specimen. At both extremities of the sample, a measurement guide is anchored in the sample in order to monitor the displacement of the sample by means of two laser displacement sensors (resolution of 0.5 μm).

5.3.2 Concrete

Measuring the thermal dilation of concrete at early ages can represent an important challenge due to the fact that: (i) volumetric methods cannot be applied in non-homogeneous 'small' samples; (ii) the size of concrete specimens causes the cooling/heating processes to take a few hours and it is very hard to get more than a few measurements in the first 24 h of age (the CTE is evolving significantly during

such measurement). Several test apparatus were developed in different laboratories for the determination of the autogenous strain and the CTE. In Table 5.1, the parameter of several test apparatus coming from the literature are presented. The main variations in the test apparatus come from:

- Dimension of the sample;
- Sample orientation (horizontal (H) or vertical (V));
- The system used to limit the friction between the mold and the specimen and to assure the sealing of the specimen;
- The thermal regulation;
- The measurement length;
- The displacement measurement system (internal or external and the sort of displacement sensor);
- The knowledge of the dilation of the test apparatus and the instrumentation (temperature compensation in the measurement);
- The temperature measurement of the sample;
- The need of sample preparation (for measurement after setting).

The dimensions of the sample are generally based on the nominal maximum diameter of the aggregate of the concrete and the length of measurement necessary to ensure sufficient measurement accuracy. In order to characterize the material since the setting or even before, the orientation of the sample is generally horizontal (ease of casting, no influence of the dead load of the specimen on the measurement). The friction between the sample and the mold is minimized by using specific material like the combination of plastic film and grease. The temperature of the concrete can be regulated by means of thermally controlled insulated mold (Koenders 1997; Lokhorst 1998; Bjontegaard 1999; Gutsch 2000; Hammer et al. 2003) or by placing the test apparatus in a environmental chamber controlled in temperature. Two types of instrumentation are used for the monitoring of the displacement: external sensor (displacement transducer) and embedded extensometer. Embedded extensometer behaves as an inclusion and should be small as possible and with a low rigidity in order to not restrain the displacement of the concrete being tested. Linear variable displacement transducers (LVDT) are the most used sensor for the measurement of concrete displacement (Boulay 2003) because of their accuracy and the fact that they are reusable. The temperature of the sample is generally measured in the center of the specimen by using a thermocouple while the temperature of the testing room is recorded only by few authors. However, when thermal variation are applied on a sample, thermal variation of the test rig occurs and should be considered for the correct determination of the CTE. Several examples of test apparatus designed for the monitoring of the autogenous strain and the coefficient of thermal expansion are shown in Fig. 5.8.

Table 5.1 Test apparatus for the determination of the CTE and the autogenous deformation

References	Sample dimension	Sample orientation	System to reduce friction and sealing	Thermal regulation	Measurement length	Displacement sensor	Temperature measurement
Koenders (1997), Lokhorst (1998)	150 × 150 × 1000 mm	H	Lubricating grease, plastic cover foil and sheet of felt	Thermally controlled insulated mould in a climate-controlled room	750 mm	4 LVDT's	3 thermocouples at mi-heigth of the sample
Gutsch (2000)	100 × 100 × 620 mm	H	2 layers of plastic foil with vaseline	Thermally controlled insulated mould in a climate-controlled room	Unknown	Quartz-glass tube or/and electric strain gauged glued	Unknown
Bjontegaard (1999), Hammer (2003)	100 × 100 × 500 mm	H	2 layers of plastic foil with talcum powder in between and an aluminium foil	Thermally controlled insulated mould in a climate-controlled room	470 mm	2 LVDT's	1 thermocouple in the center of the specimen
Kada et al. (2002)	100 × 100 × 400 mm	H	The sample is wrapped in plastic bags	The sample is immersed in a heat-controlled water bath	Unknown	Vibrating wire extensometer embedded in the sample	Temperature recorded at the center of the sample with the vibrating wire extensometer

(continued)

Table 5.1 (continued)

References	Sample dimension	Sample orientation	System to reduce friction and sealing	Thermal regulation	Measurement length	Displacement sensor	Temperature measurement
Cusson and Hoogeveen (2006, 2007)	75 × 75 × 295 mm	H	A layer of vaseline and a thin plastic film	Environmental chamber	Unknown	2 LVDT's	1 thermocouple in the center of the specimen and 1 thermocouple in the environmental chamber
Yeon et al. (2013)	Ø: 75 mm, h: 237.5 mm	H	A single layer of soft fabric (radial direction) and a styrofoam (longitudinal direction)	/	153 mm	Embedded vibrating wire strain gage	A thermistor is integrated to the displacement sensor
Viviani et al. (2006, 2007)	Ø: 315 mm, h: 1000 mm	V	/	/	800 mm	Embedded fibre-optic sensor	2 thermocouples (at the center and the extremity)

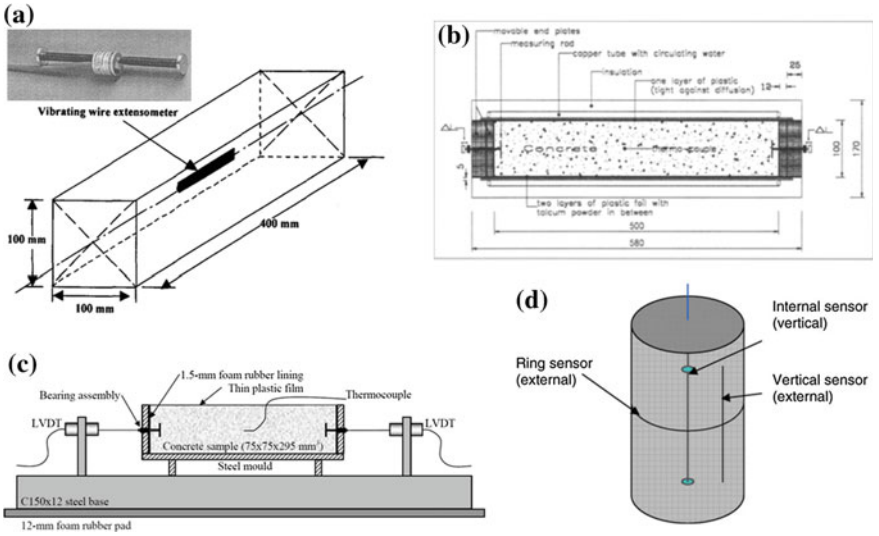

Fig. 5.8 Examples of test apparatus designed for the monitoring of the autogenous strain and the coefficient of thermal expansion, **a** Kada et al. (2002), **b** Bjøntegaard et al. (2015), **c** Cusson and Hoogeveen (2007) and **d** Viviani et al. (2007)

5.4 Test Protocol and Data Treatment

5.4.1 Review of the Literature

As explained by Boulay (2003), several authors have developed different methodologies to assess the CTE and the autogenous strain. A first method is based on the removal of the autogenous deformation by differences between two samples subjected to two histories of temperature. The maturity of both samples is considered when autogenous deformations are eliminated (Laplante and Boulay 1994). For consideration of the ageing and the main temperature effect, concrete properties can be expressed in function of the equivalent time t_{eq} (Eq. 5.4). Equivalent time is based on the Arrhenius equation and is function of the age of the material t, the evolution of the temperature T (°C), a reference temperature T_r (here 20 °C), the universal gas constant R (=8.314 J/mol/K) and the apparent activation energy E_a (J/mol).

$$t_{eq}(t, T) = \int_0^t \exp\left(\frac{E_a}{R} \cdot \left(\frac{1}{273 + T(s)} - \frac{1}{273 + T_r}\right)\right) \cdot ds \tag{5.4}$$

However, the temperature has an effect on the evolution of the autogenous deformation and the CTE. Thus it is needed to have very close temperature histories which lead to a lack of accuracy in the determination of the CTE (Boulay 2003).

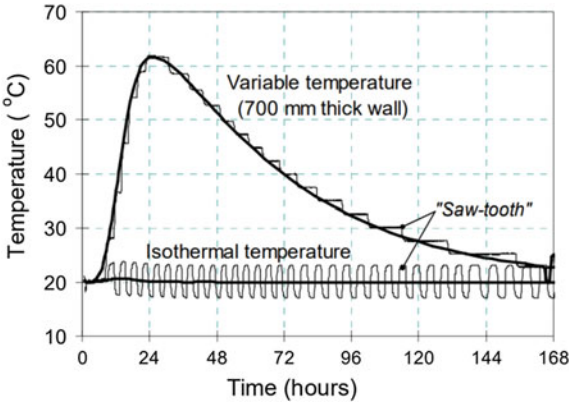

Fig. 5.9 Test procedures proposed by Hammer and Bjøntegaard (2006) for the characterization of the autogenous strain and the CTE

The second method uses only one sample on which thermal variations are applied (Bjøntegaard et al. 2004). The test procedure is based on the repeated application of thermal variation around a constant temperature (isothermal condition) or around a variable temperature (non-isothermal condition). Hammer and Bjøntegaard (2006) recommend imposing thermal variations as fast as possible in order to reduce the amount of autogenous deformation taking place during the thermal variation. The amplitude of the thermal variation should be high enough to insure a good accuracy in the determination of the CTE and small enough in order to reduce the influence of the temperature in the determination of the CTE. However, no specific value was provided for the frequencies and the amplitude of the thermal variation. An example of test procedure in isothermal and non-isothermal condition is shown in Fig. 5.9.

As presented by Delsaute and Staquet in (2017a), several protocols and mathematical treatments were developed for the determination of the CTE. In Table 5.2, the parameter of several test protocols coming from the literature are presented. The main variations in the test protocol come from:

- The amplitude of the thermal variation (ΔT)
- The duration of the isothermal phase (Δt)
- The nature of the material tested [cement paste (CP), mortar (M) or concrete (C)]
- The evolution of the temperature between the different cycles.

No specific recommendation is provided in the literature for the calculation of the CTE. When applying repeated thermal variation on a sample, the CTE was generally computed for hardened concrete by using Eq. 5.5 in which ε_{tot} is the total strain measured, α_{ta} is the CTE of the test apparatus and ΔT is the thermal variation applied. This method has the disadvantage to not consider the autogenous strain development of the sample during the thermal variation. In case of a decrease/increase in temperature of the sample when the specimen is shrinking, an overestimation/underestimation of the CTE is done which is especially significant at very early age.

$$\alpha_{\mathrm{T}}(\mathrm{t}) = \frac{\varepsilon_{tot} - \alpha_{ta} \cdot \Delta T}{\Delta T} \tag{5.5}$$

Table 5.2 Parameters of test protocols for the determination of the CTE and the autogenous deformation by using only one sample (Delsaute and Staquet 2017a)

References	ΔT, °C	Δt, min	Kind of device	Remark
Loser et al. (2010), Wyrzykowski and Lura (2013a, b)	6	90	Volumetric (CP and M)	Trapezoidal variation
Cusson and Hoogeveen (2006, 2007)	5	240	Linear (C)	
Ozawa and Morimoto (2006)	7	N.A.[a]	Linear (C)	Sinusoidal variation
Maruyama and Teramoto (2011, 2012), Maruyama et al. (2014)	5	25	Linear (CP and M)	Isothermal and various temperature histories with alternated triangular variation
Bjøntegård and Sellevold (2001)	6	120	Linear (C)	

[a]N.A. = not available

To overcome this issue, Maruyama and Teramoto (2011) have developed a test protocol presented in Fig. 5.10a for cement paste and mortar. Four thermal variations of 5 °C are applied in 100 min on a sample. The coefficient of thermal expansion is defined as the average slope between the sample strain and the temperature during the four thermal variations (Fig. 5.10b) and corresponds to the midpoint age of the 4 thermal variations. To decrease the fluctuation in the results, only results between a thermal variation of 0.5 and 4.5 °C is considered for the computation of the CTE. Such calculation reduces the influence of the autogenous strain in the determination of the CTE. However, such calculation method makes the assumption that the evolution of

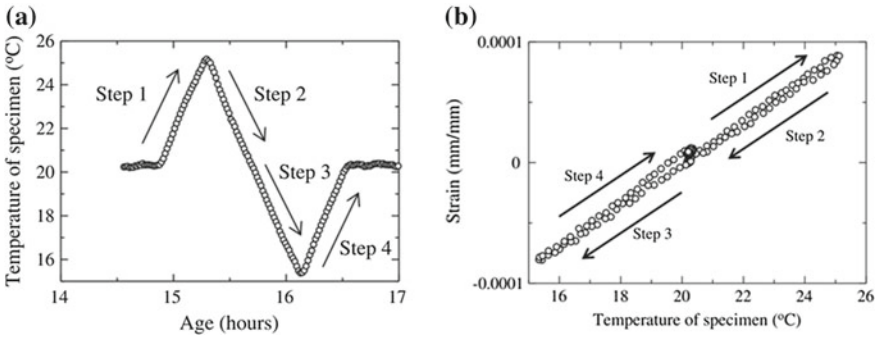

Fig. 5.10 Scheme of determination of the coefficient of thermal expansion of Maruyama and Teramoto (2011), **a** representative evolution of the temperature during thermal variations, **b** evolution of the temperature—strain relationship when thermal variations are applied

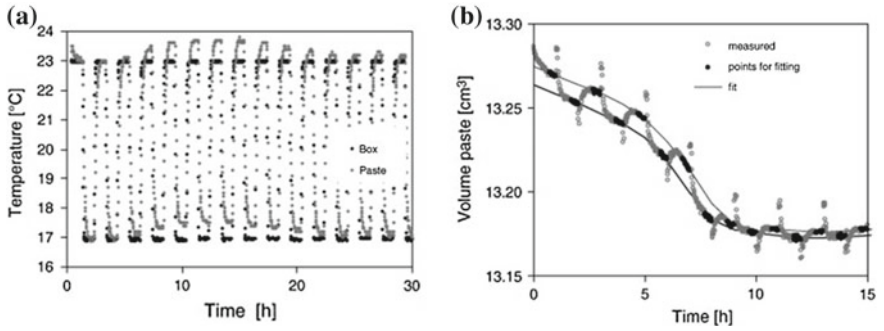

Fig. 5.11 Scheme of determination of the coefficient of thermal expansion of Loser et al. (2010), **a** representative evolution of the temperature, **b** evolution of the volume of the paste when thermal variations are applied

the autogenous strain is linear during the thermal variations which still induces small error in the determination of the CTE.

To solve this problem, the non-linear development of the autogenous strain should be considered in the calculation of the CTE. On cement paste and mortar, Loser et al. (2010) have applied repeated thermal variations of 6 °C (between 17 and 23 °C) since casting (Fig. 5.11a). Only data obtained at the end of each plateau of temperature (when no thermal gradient is assumed in the sample) have been considered (Fig. 5.11b). By means of cubic smoothing splines, two encasing envelopes of the volume of the paste are defined for a curing temperature of 17 and 23 °C. The CTE is then defined by knowing both the difference in volume and temperature between the two envelope curves. An example of such treatment is presented in Fig. 5.11 for volumetric method (Loser et al. 2010). This method has the disadvantage to not consider the maturity of the sample. During thermal variation, an acceleration or deceleration of the hydration process is induced. For a good consideration of the maturity of the sample, strain should be considered according to the equivalent age (Eq. 5.4).

Recently, Zhutovsky and Kovler (2017) have developed a new methodology based on ultrasonic pulse velocity measurement for the assessment of the coefficient of thermal expansion. The calculation of the CTE is based on poromechanics theory. This approach has the advantage of defining the CTE without having to perform a decoupling with the autogenous strain. However, this method does not consider the self-desiccation of the material and thus the increase of the coefficient of thermal expansion which leads to an underestimation of the CTE after the final setting of the cement paste.

5.4.2 *Development of a New Test Protocol for Concrete*

At the concrete scale, no specific data treatment associated to a test protocol was presented in the literature to properly define the development of the CTE and the autogenous strain since setting. For that reason, the development of a new experimental protocol and a new mathematical analysis strategy were defined to characterize the autogenous deformation and the coefficient of thermal expansion during the same single test at the Université Libre de Bruxelles (Delsaute and Staquet 2017a). This new methodology considers correctly the evolution of the autogenous strain when thermal variations are applied to the sample since the setting.

The free strains of the concrete or mortar are measured from casting using the BTJADE (from the French acronym 'BéTon au Jeune Age, Déformation Endogène') device (Boulay 2012). The test rig (Fig. 5.12) is composed of a vertical flexible corrugated PVC mold to monitor the free strain and fixed metallic parts. The whole frame is placed in a temperature controlled bath and is designed to accommodate 3 tests rigs simultaneously. The sensors for each channel are the central displacement, the temperature of the sample with a thermocouple, the temperature of the surrounding water in the tank with a platinum probe and the temperature in the air above the cover of the tank, near the displacement transducer, with a platinum probe also. For a good consideration of the heterogeneity of the concrete, the diameter of the cylinder has to be greater than the coarse aggregate (a factor 5 is a minimum). For that reason, a diameter of 125 mm is used. The base length of the sample is approximately 225 mm. More details about the BTJADE are given in Boulay (2012).

When measurements are done, free strain of the concrete is defined by removing the influence of the temperature variations itself inside the tank and the influence of the temperature of the room on the displacement transducer located above the cover of the tank. As the test is carried out in sealed condition, the free strain corresponds to the sum of the autogenous strain and the thermal strain. Therefore the total strain of the concrete ε_{tot} (m/m) is defined as:

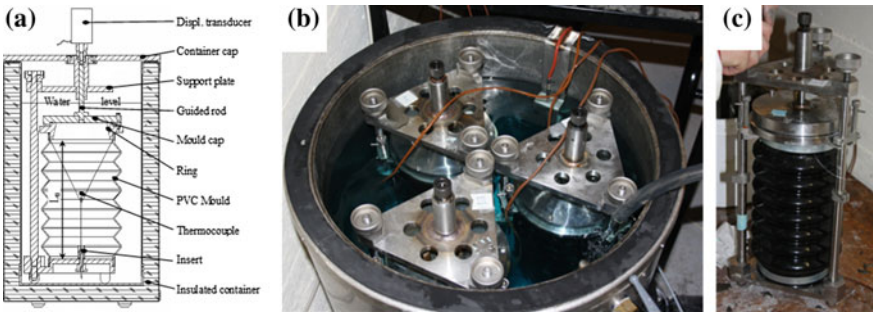

Fig. 5.12 BTJADE test set up (Delsaute and Staquet 2017a)—section of the whole test setup (**a**), water tank with three tests rigs (**b**), test rig before introduction in the water tank (**c**)

$$\varepsilon_{tot} = \varepsilon_{au} + \alpha_c \cdot \Delta T_c = \frac{\Delta L}{L_0} - \alpha_{wt} \cdot \Delta T_{wt} - \alpha_{at} \cdot \Delta T_{at} \tag{5.6}$$

where ΔL is the displacement measured by the displacement sensor (mm), ε_{au} is the autogenous strain (m/m), α_c is the coefficient of thermal expansion of the concrete (m/m/°C), ΔT_c is the thermal variation of the concrete, the index wt is related to the thermal variation of the water in the tank and the index at is related to the thermal variation of the air above the cover of the tank. The thermal dilation coefficient of the test rig α_{wt} and α_{at} are defined by replacing the concrete sample by a stainless steel rod whose the coefficient of thermal expansion is well known. α_{wt} is determined with a room temperature constant and steps of temperature imposed to the water inside the tank. α_{at} is obtained with a constant temperature of the water inside the tank and steps of temperature imposed to the air of the room (Boulay 2012).

The base length of the sample is approximately 225 mm and the inner diameter 125 mm. When measurements are done, the free strain of the concrete is defined by removing the influence of the temperature variations themselves inside the tank and the influence of the temperature of the room on the displacement transducer located above the cover of the tank. As the test is carried out in sealed condition, the free strain corresponds to the sum of the autogenous strain and the thermal strain.

At the basis the test rig has been design for the monitoring of the autogenous strain. In order to validate the test apparatus, results coming from a horizontal testing device has been compared as presented in (Delsaute et al. 2016). A general very good agreement was observed between both results.

The test protocol is based on repeated thermal variations which are applied since the casting of the sample. The thermal variations are designed by optimizing the three following parameters: the duration of the temperature increase, the thermal variation amplitude and the duration of the isothermal phase in the tank. The duration of the temperature increase in the tank must be as fast as possible in order to minimize concrete autogenous deformation amplitude between two sets of measurements and to maximize the number of thermal variation at early age when the CTE evolve significantly. The thermal variations amplitude must be high enough to allow measuring significant displacement (digital displacement transducer with accuracy of 1 µm over the whole stroke) and small enough in order to reduce the influence of the temperature variation on the development of the autogenous strain (Jensen and Hansen 2001). The duration of the isothermal phase in the tank must be high enough to avoid any thermal gradient inside the concrete sample at the end of the plateau of temperature.

Several preliminary tests were performed on hardened concrete with the BTJADE device in order to optimize these parameters. The test protocol is presented in Fig. 5.13. The recording of data provided by each thermal and displacement sensor is done every minute. The phase of temperature change is limited to 10 min; the magnitude of the temperature variation is ±3 °C and the duration of the isothermal phase is 150 min. The duration of the isothermal phase can be adapted according to the composition. For composition with high thermal conductivity, temperature stabilization in the concrete is already reached after 120 min. At this period, an identical

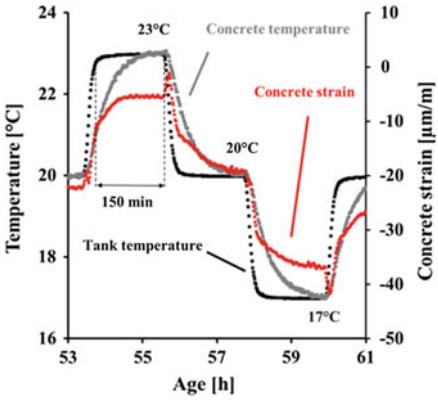

Fig. 5.13 Preliminary test on hardened concrete

temperature is measured in the tank and in the concrete sample for hardened concrete as shown in Fig. 5.13. As the thermal inertia of the test rig is lower than the one of the concrete sample, a faster change in temperature takes place in the test rig. This induces an error in the computation of concrete strain (Eq. 5.6) when the temperature of the water changes in the tank. This is observed in the evolution of the concrete strains in Fig. 5.13 at the beginning of each thermal variation.

Therefore no thermal gradient occurs at the end of the plateau of temperature. 10 cycles were performed on this hardened concrete for which it is assumed that no significant autogenous strain occurs (the age of the sample was higher than one month at the start of the test). Results of the CTE are presented in Fig. 5.14. An average value of 11.6 µm/m/°C is obtained. The minimal value is 11.1 µm/m/°C and the maximal value is 12.0 µm/m/°C. The standard deviation is very low and is equal to 0.3 µm/m/°C which corresponds to 2.3% of the average value of the CTE. Through these results, it is concluded that such protocol is accurate enough for the assessment of the CTE on hardened concrete. As the variation of the thermal conductivity with aging of concrete is limited (De Schutter and Taerwe 1995; Briffaut et al. 2012), it is assumed that no thermal gradient occurs because of the temperature variation in

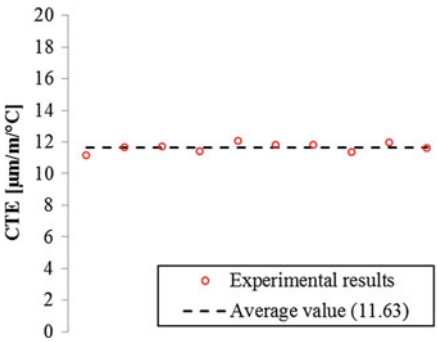

Fig. 5.14 Results of the CTE for a hardened concrete

the tank during the hardening process of the concrete. The thermal gradient due to the hydration is assumed to be unchanged.

This last assumption is verified on an ordinary concrete on which two tests was performed with different temperature histories. The composition of the concrete is presented in the references (Boulay et al. 2014). For the first test, a constant temperature of 20 °C is imposed. The second test uses the protocol of temperature illustrated previously in Fig. 5.13. For each test, two test rigs are used in order to assure the repeatability of the results. For a good comparison, both tests use a concrete coming from the same batch. The scheme of the experiment is presented in Fig. 5.15.

The test starts approximately 1 h after mixing. Results related to the evolution of the temperature at early age are presented in Figs. 5.16 and 5.17. Figure 5.16 shows the evolution of the temperature in the water tank and inside the sample. For each thermal variation, the temperature of the sample reaches the temperature imposed by the thermal regulation. At the end of the plateau of temperature, the temperature is stable in the sample. In Fig. 5.17, the temperature inside samples from both tests is compared. Moreover the comparison is extended to two additional curves which correspond to the temperature of the sample with a constant thermal cure of 20 °C

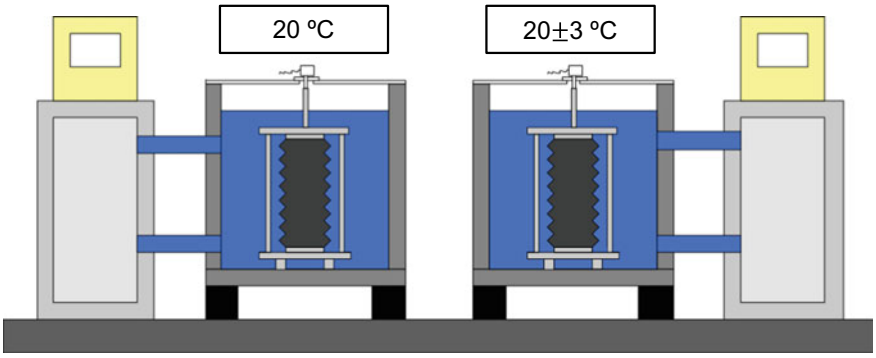

Fig. 5.15 Scheme of the experiment

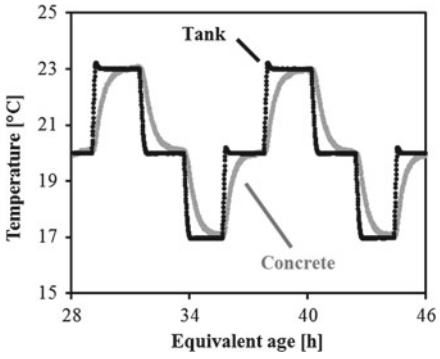

Fig. 5.16 Thermal variation in the water tank and inside the sample

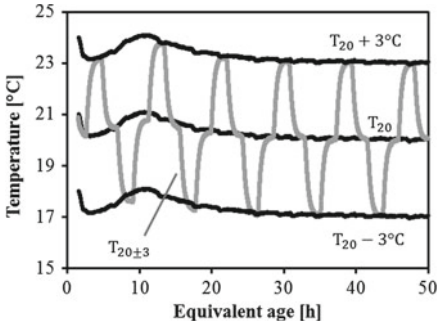

Fig. 5.17 Evolution of the temperature of the sample for both tests

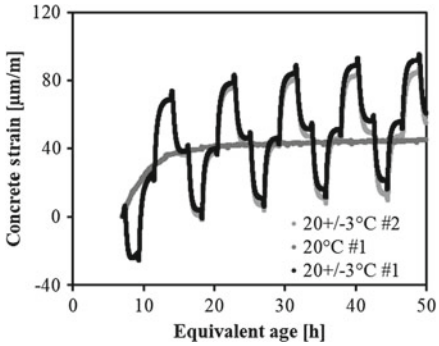

Fig. 5.18 Evolution of the total strain for both temperature histories

on which an addition or a subtraction of 3 °C is operated. For each end of plateau of temperature, a very good correspondence of the temperature is obtained between both tests. This very good correspondence is also observed during the peak of hydration occurring the first 24 h. It is therefore concluded that the thermal variations cause no significant change in the thermal gradient due to hydration.

The total concrete strains from both tests are compared in Fig. 5.18 since final setting time. Results obtained at the end of the plateau of temperature at 20 °C are very close to the results obtained at a constant temperature of 20 °C. It is therefore possible to fit results obtained at the end of the plateau at 20 °C in order to define the total strain obtained for a cure at 20 °C. The same methodology can be used to define the free strain at 17 and 23 °C. In Fig. 5.19, the temperature and the total strain in the sample with repeated thermal variation are compared. A good coherence between both evolutions is observed. At the beginning of each thermal variation, a discontinuity in the evolution of the total strain is observed. This discontinuity comes from the computation of the total concrete strains. When the displacement induced by the dilation/contraction of the test rig is removed from the total measurement, it is assumed that each component of the test rig has an instantaneous thermal response. The thermal inertia of each component is not considered. That is why such variations in the computed total concrete strains are observed. Therefore only results obtained at the end of the plateau of temperature have a physical meaning.

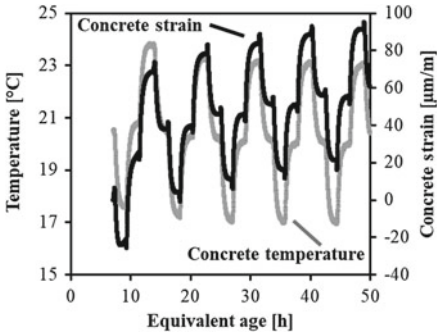

Fig. 5.19 Evolution of the total strain and the temperature for the test with repeated thermal variations

The coefficient of thermal expansion (CTE) and the autogenous strain are computed in several steps. First the concrete strain is defined by removing thermal displacement of the test rig (an acquisition is carried out each minute). Then only physical values of the total strain are considered. This physical value corresponds to the moment when the test rig and the concrete have no thermal gradient and have a constant temperature. This moment corresponds to the end of the plateau of temperature. An average value of the last five data recorded during the plateau in temperature is considered in order to reduce the noise coming from the measurement of the temperature and the displacement sensors. To define the autogenous strain and the CTE, it is needed to have two temperature histories. For that purpose, a fictive temperature history is created by considering only the values obtained during the plateau of temperature at 20 °C. With a spline interpolation, it is possible to create new data (total strain and temperature) which correspond to a constant cure at 20 °C. Therefore a predictive value of the total strain and temperature is obtained for a constant temperature of 20 °C in the tank. For both temperature histories, the variation of the total strain, the autogenous strain and the thermal strain between two plateaus of temperature is given in Eq. 5.7.

$$\Delta\varepsilon_{tot} = \Delta\varepsilon_{au} + \alpha_c \cdot \Delta T \tag{5.7}$$

The effect of the temperature on the evolution of the autogenous deformation and the CTE (Bjøntegaard 2011) was previously demonstrated by several authors. However the difference of evolution was highlighted for a very large difference of temperature. For a very small difference of temperature, as here 3 °C, the effect of the temperature on the evolution of the autogenous deformation and the CTE is very low. In consequence it could be considered that, for both temperature histories, the evolution of the autogenous strain during 150 min and the value of the CTE is the same. Therefore, with value of the thermal variation and total strain variation for both temperature histories, the CTE is defined as expressed in Eq. 5.8. In this equation, the index 1 and 2 are relative to the two different temperature histories.

$$\alpha_c = \frac{\Delta\varepsilon_{tot,1} - \Delta\varepsilon_{tot,2}}{\Delta T_1 - \Delta T_2} \tag{5.8}$$

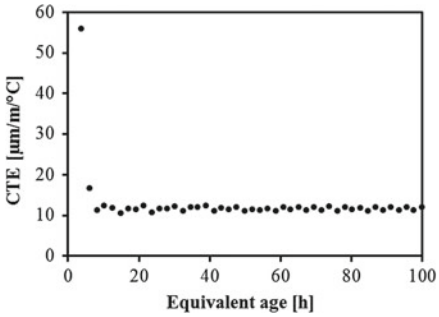

Fig. 5.20 Evolution of the coefficient of thermal expansion according to the equivalent age

Results of the CTE are given in Fig. 5.20. The CTE changes strongly during the few first hours after casting till an age of 8 h. Afterwards, the CTE follows a very constant value. The age when this change takes place corresponds to the setting of the concrete. This observation was already done by Loser et al. (2010) for cement paste and by Delsaute and Staquet (2017a) for concrete. For this composition, the CTE seems very constant after setting. This is in coherence with results obtained in the literature on ordinary concrete. Indeed, for concrete with a high water-cement ratio, no strong variation of the CTE occurs because the value of the relative humidity stays high during the whole hydration process. Figure 5.21 presents only results of the CTE obtained after setting. The scattering in the results is very low. However just after setting a higher scattering is observed. It is due to the strong increase of the autogenous strain during this period. An average value of 11.6 µm/m/°C is obtained for the CTE.

When the CTE is defined, the evolution of the autogenous deformation is defined with the removal of the thermal strain on the total strain (Eq. 5.7). Figure 5.22 presents the evolution of the autogenous strain by considering a constant value of the CTE of 11.6 µm/m/°C. Results are strongly dependent on the time when the autogenous strains are initialized. In order to correctly compare results, each curve is initialized at an equivalent age of 140 h (Fig. 5.23). Results from both tests give very equivalent results and show a very good repeatability.

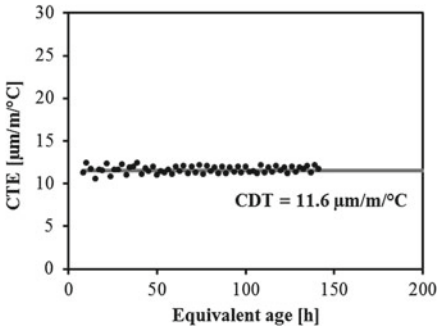

Fig. 5.21 Evolution of the coefficient of thermal expansion after setting

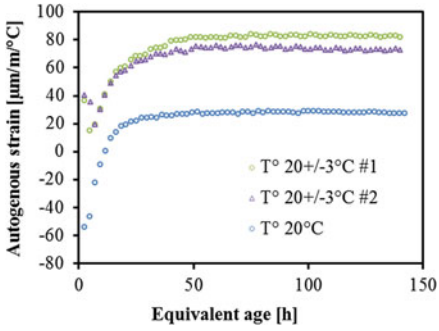

Fig. 5.22 Autogenous strain

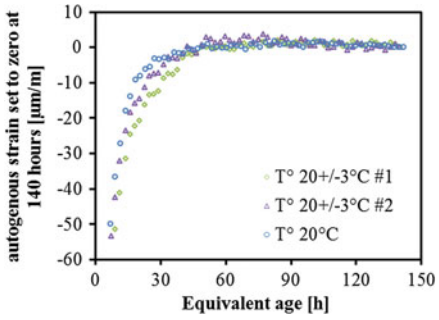

Fig. 5.23 Normalized autogenous strain at 140 h

It is then concluded that the new methodology developed here is able to monitor the evolution of the CTE and the autogenous strain since setting in one single test. The general scheme of the test protocol and the treatment of the results is presented in Fig. 5.24.

5.5 Investigations and Results

5.5.1 Sensitivity Analysis on the Determination of the CTE Induced by the Data Processing

As presented above, different methodologies have been developed and used in the past for the determination of the CTE since casting. At very early age, the CTE is very sensitive to how the data are processed. To illustrate and quantify the importance of the treatment of the data, the coefficient of thermal expansion of a concrete was computed by using six different methods.

The first method does not consider the evolution of the autogenous strain taking place during the thermal variation. The second method is inspired from the work

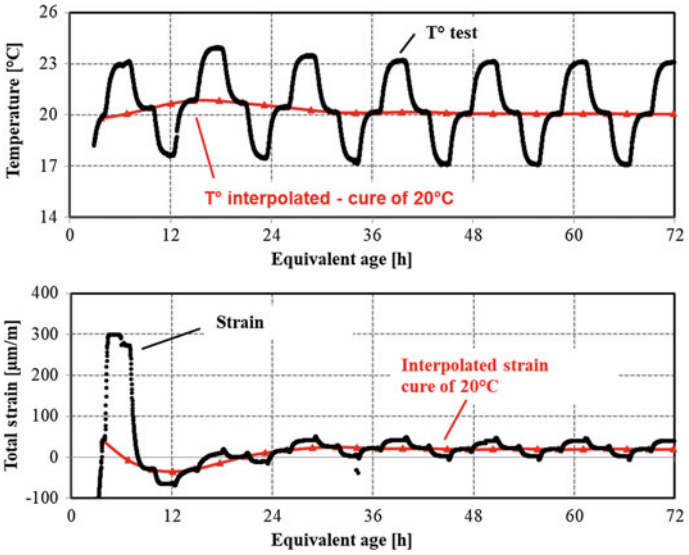

Fig. 5.24 Evolution of the temperature and the concrete strain during the test (Delsaute and Staquet 2017a)

of Maruyama and Teramoto (2011) for which the slope between the strain and the temperature of the concrete is computed between 10 and 90% of the thermal variation in order to define the CTE. Third, the method developed by Loser et al. (2010) has been adapted to the testing methodology developed at ULB. Three envelope curves considering data at 17–20 and 23 °C were computed as by Loser et al. (2010). The computation of the CTE has been carried out as the average of the CTE obtained between each envelop curve and the maturity of the sample was not considered in the computation. Ultimately, the novel method presented in this chapter was used with three sorts of interpolation: linear interpolation (method 4), spline interpolation (method 5) and Piecewise Cubic Hermite Interpolating Polynomial (PCHIP (Fritsch and Carlson 1980)—method 6). The studied concrete is a Very High Performance Self-Compacting Concrete (VHPSCC) which was designed in 2005 (Staquet et al. 2005) for pre-cambered beams. The decoupling between the autogenous and thermal strain is very complex for such composition due to the fast and intense development of the autogenous strain during the first 24 h after setting (Roziere et al. 2015).

In Fig. 5.25, the development of the CTE computed with each method is presented according to the equivalent age. These results correspond to the average obtained from measurement performed on 2 samples. The general trends observed are the same for each method. A strong decrease of the CTE is observed during a short period which is related to the setting of the material. At an age of around 15 h, the CTE reached a minimum and then increases slightly. Till an age of 20 h, the development of the CTE is significantly different according to the method used for the data processing. This is highlighted in Fig. 5.26 in which only results obtained before an equivalent age of 30 h

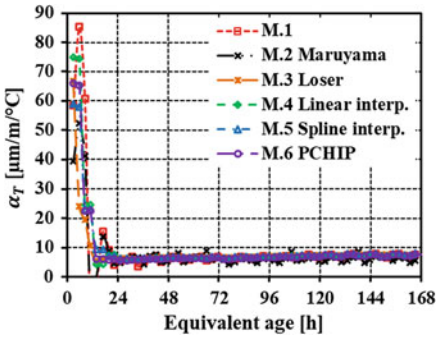

Fig. 5.25 Comparison of 6 methods for the determination of the CTE

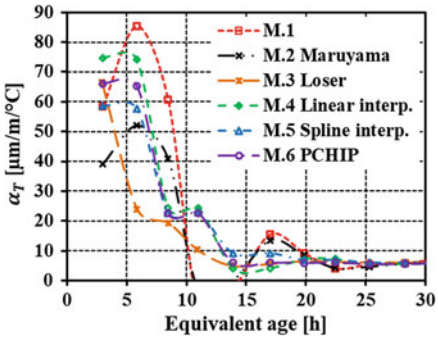

Fig. 5.26 Zoom during the first 30 h of the Fig. 5.25

are shown. In addition, in Fig. 5.27, the development of the autogenous strain and the autogenous strain rate is presented. CTE results got with the first and second methods show quite different trends in comparison to other methods of data processing. An increase and then a significant decrease of the CTE are calculated during the first 10 h. Negative CTE values are obtained between an equivalent age of 10 and 15 h. These non-physical variations are related to the non-consideration of autogenous deformations in the treatment of the results. Indeed, during this time interval, the autogenous strain rate is very intense (Fig. 5.27). When calculating the CTE, the

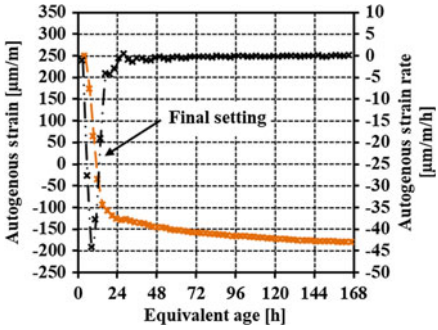

Fig. 5.27 Development of the autogenous strain and the autogenous strain rate

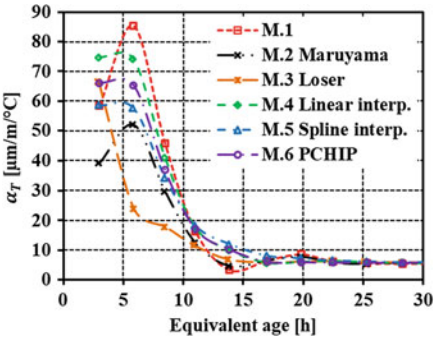

Fig. 5.28 Evolution of the CTE with the use of moving average on 4 points

concrete deformations due to temperature variations are underestimated during an increase in temperature and overestimated during a decrease in temperature. This underestimates and overestimates respectively the value of the CTE. The influence of the maturity of the concrete sample on the determination of the CTE is then studied with the third method. A faster decrease of the CTE is observed during the first 15 h. Then the value of the CTE is similar to the value obtained with the other methods. The influence of the interpolation method is studied with the methods 4–6. For each method, very similar value of the CTE is obtained after an age of 6 h and the decrease of the CTE takes place between an age of 6 and 15 h. Significant difference in the amplitude of the CTE between the three methods is only observed during the 20 first hours after casting.

The error in the computation of the CTE induced by the data processing used for the removal of the autogenous strain is reduced by applying 4 points moving average method on data obtained after the induction period (Fig. 5.28). It is generally observed that the spread in the results obtained is minimized and especially between an equivalent age of 10 and 20 h. No negative value of the CTE is then computed with the method 1 and 2. The early decrease of the CTE is still observed with the method 3.

The importance of the data processing in the determination of the coefficient of thermal expansion is quantified with the computation of the relative difference in the evolution of the CTE between the 6 methods. For each thermal variation, the mean value of the CTE obtained with the 6 methods of data processing $\alpha_{T,m}$ is computed. The relative change in the evolution of the CTE is given in Fig. 5.29. A maximal relative change of around 60% is obtained with the first and the second method at an equivalent age of 14 and 6 h respectively. At very early age, the relative difference is generally lower for the method 6. For later ages, a very limited relative difference is obtained with each method except for the method 2. The origin of this divergence comes from the difference of thermal inertia between the test rig, the tank and the concrete sample. Concrete strains are computed according to Eq. 5.6 for which it is assumed that the thermal dilation of the test apparatus occurs directly when thermal variation are applied. With such computation, it is not possible to correctly define the concrete strain when the temperature of the water in the tank changes. Therefore, the

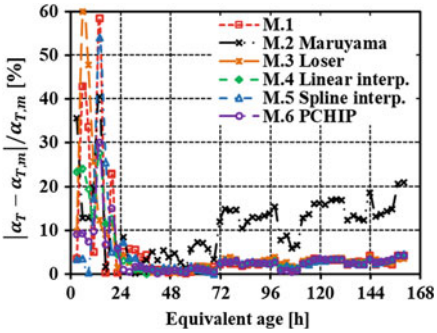

Fig. 5.29 Relative difference in the evolution of the CTE with the different method of data processing

second method of data processing cannot be used for the computation of the CTE at early age and at later ages. Such method can only be used if the concrete strains are well defined when the temperature varies. The use of this method leads here to an underestimation of the CTE during the hardened stage. In addition, for each method, the standard deviation s is computed according to Eq. 5.6 where N is the number of thermal variation applied during the test.

$$s = \sqrt{\sum_{i=1}^{N} \frac{\left(\alpha_T(t_i) - \alpha_{T,m}(t_i)\right)^2}{N}} \tag{5.9}$$

The standard deviation is given in Fig. 5.30 for data got till an equivalent age of 30 or 160 h. The methods developed for cement paste and mortar (methods 2 and 3) have higher standard deviation. This highlights the higher scattering in the results obtained when the autogenous strain development and the maturity of the concrete are not considered accurately. In addition, as presented by Loser et al. (2010), how concrete strains are interpolated when thermal variations are applied has a significant impact in the determination of the CTE. It is observed that the use of PCHIP decreases the standard deviation in comparison to linear interpolation and spline interpolation especially at early age. In conclusion, the method 6 of data

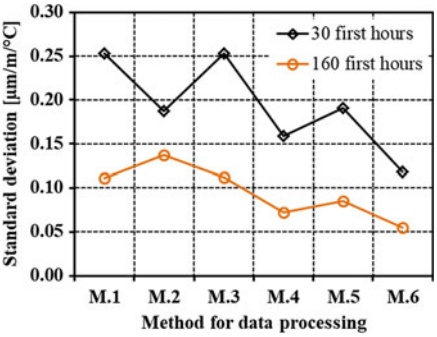

Fig. 5.30 Standard deviation of the CTE obtained with each method for test duration of 30 h and 168 h

processing is recommended for the determination of the CTE and the autogenous strain when thermal variations are applied on a sample.

5.5.2 *Extension to Cement Paste and Mortar Scale*

For the study of the multiscale aspect of the free deformation, a similar strategy has been developed for the monitoring of the CTE and the autogenous strain of cement paste and mortar. As presented in the Sect. 5.3.1, several devices were developed for the monitoring of the autogenous strain. One of the most used at the cement paste and mortar scale is the Autoshrink device developed by Mejlhede Jensen and Freiesleben Hansen (1995). A thermal regulation has been designed in order to apply thermal variations on the test rig (Milenkovic et al., no date; Delsaute 2016; Königsberger et al. 2018). The temperature of the sample is controlled by a flow of a specific liquid for thermal regulation circulating in a convolution system which surrounds the Autoshrink device. In order to improve the efficiency of the thermal regulation, the whole system is surrounded by a box with thermal insulation which limits exchanges with the ambient environment. The equipment is located in an air-conditioned room with a control system of the temperature and the humidity. The thermal regulation and the Autoshrink device are presented in Fig. 5.31. A thermal calibration of the whole test rig has been carried out by using a stainless steel rod for which the CTE is known. For the measurement of the displacement and the temperature, a Solartron network is used. It is composed by three displacement sensors Solartron LE2 and two temperature sensors. A thermocouple is used to monitor the temperature of one sample (embedded in the centre at mid-length) and one PT100 is used to monitor the temperature of the air inside the convolution system.

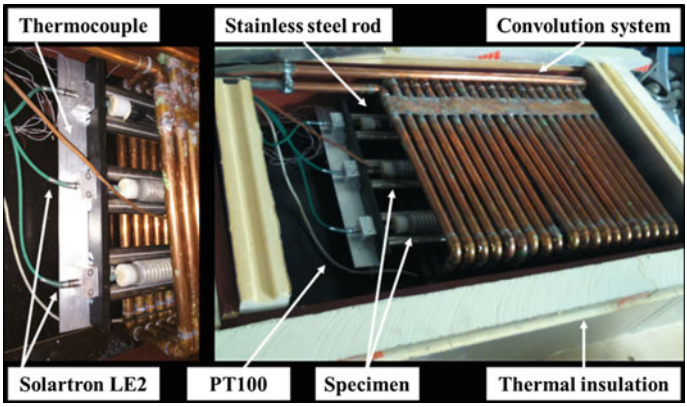

Fig. 5.31 Autoshrink device with thermal regulation developed at ULB (Delsaute 2016)

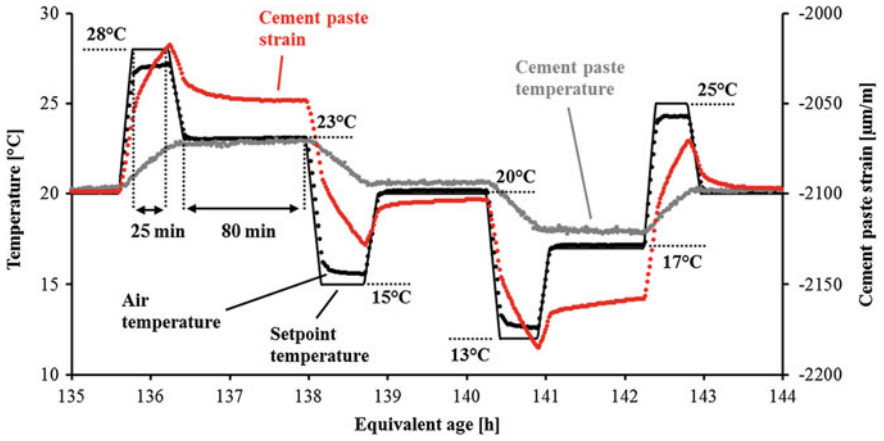

Fig. 5.32 Test protocol for cement paste and mortar with Autoshrink device

The thermal regulation is not performing as the one in the BTJADE system. For that reason, some adaptations have been made to the test protocol (Fig. 5.32). A first thermal variation of ± 8 °C is applied in 10 min. The temperature is kept constant during 25 min. Then a thermal variation of ∓ 5 °C is applied in 10 min. Finally the temperature is kept constant during 80 min. The final magnitude of the temperature variation is ± 3 °C and the duration of the isothermal phase is 80 min. Temperature stabilization in the cement paste or mortar is well reached after 80 min as shown in Fig. 5.32.

5.5.3 Correlation Between the Early Development of the CTE and the Autogenous Strain and the Setting

The setting period is commonly defined according to the results of penetration tests on cement pastes or mortars and corresponds to a progressive coalescence of a continuous path of hydrates. At the beginning of this period (initial setting), the concrete stiffness is almost inexistent while, at the end of this period (final setting), the concrete starts to stiffen (Hansen 2011). Correlations between the early development of the CTE, the autogenous strain and the setting had been made by several authors. Remarkable points were observed by different authors. Sant et al. (2006) have shown that final setting time can be defined using the rate of autogenous strain development in a cement paste. The final setting time was identified as the minimum of the derivative of the autogenous strain. Several authors (Loser et al. 2010; Wyrzykowski and Lura 2013a, b) have also associated the final setting time with the start of the decrease of the CTE from the liquid to the solid phase in cement paste. Delsaute and Staquet (2017a) have compared the evolution of the CTE and the autogenous strain to the initial and final setting obtained with penetration resistance [according to ASTM C304

standard (ASTM C403 2008)] and with ultrasonic measurement using P-wave and S-wave (Carette and Staquet 2015; Mohamed et al. 2017) for concrete composition with different W/C ratio and different type of binder. For each composition, the initial setting time has been associated to the moment when the value of the CTE does not correspond anymore to a liquid. The final setting time is associated to a minimum of the autogenous strain obtained before the swelling of the concrete. This value corresponds to a zero value of the derivative of the autogenous strain. Therefore, results of the autogenous strain and the CTE obtained by means of repeated thermal variation could be used for the determination of the initial and final setting time. However, the duration between two thermal variations must be reduced strongly at very early age in order to define both parameters accurately.

5.5.4 Further Recommendation for the Monitoring of the CTE and Autogenous Strain at Very Early Age

When the rate of the free strain is very high, as it is the case before (chemical shrinkage) and after (autogenous strain) setting, the computation of the CTE and the autogenous strain is very sensitive to how the data are processed (Sect. 5.5.1). To override this problem it is recommended to apply thermal variation faster at very early age even if their amplitude is lower in order to get a faster stabilization of the temperature in the sample. This will reduce the influence of the method used to treat the data. In addition, this will improve the assessment of the initial and final setting time. After this period, thermal variations of ±3 °C each 160 min allow defining accurately the development of the autogenous strain and the CTE.

5.6 Conclusion and Outlook

The volume changes of cementitious materials in sealed conditions are governed at early age by the evolution of the coefficient of thermal expansion (CTE) and the autogenous strain. The most recent advances on the physical mechanisms associated to their development are reported. The recent devices and test protocols developed for the simultaneous monitoring of the coefficient of thermal expansion and the autogenous strain at three different scales (cement paste, mortar and concrete) are also presented. The general testing methodologies bear some similarities but major differences remain in the test set up designs, in the testing processes and also in the data processing. Based on the physical mechanisms, existing test facilities and test protocols, a new test protocol and its associated data processing has been developed for the monitoring of the autogenous strain and the CTE. This new methodology consists to apply repeated thermal variation of ±3 °C each 160 min on a concrete

sample with the device so-called BTJADE. Thermal and autogenous strains are distinguished by creating a fictive thermal cure at 20 °C from the experimental results by using interpolation method and by considering the maturity of the sample. A sensitivity analysis has been performed in order to highlight the importance of the consideration of the autogenous strain, the maturity of the sample and how data are interpolated between thermal variations in the determination of the CTE. The use of Piecewise Cubic Hermite Interpolating Polynomial is recommended for the interpolation of the concrete strain between thermal variations. An adaptation of this new testing methodology has been presented with the Autoshrink device for cement paste and mortar. Finally, recommendation on the test protocol and the data processing are proposed for the determination at very early age of the autogenous strain, the CTE and the initial and final setting time.

The new testing method based on repeated thermal variation is a field that can offer much to the characterization of cement-based materials especially for the characterization of cement based materials composed of new raw materials (e.g. recycled aggregate, fibres and geopolymer). A lot of meaningful research efforts have emerged recently showing the capability of this new testing methodology to define with one test the initial and final setting time, the autogenous strain and the CTE. However these works were limited to laboratory temperature condition (20 °C), binder composed of mainly ordinary Portland cement and sealed condition. Therefore suggestions for future research include:

- the measurement of the internal relative humidity of the sample,
- the optimization of the time duration and amplitude of the thermal variation according to the maturity of the material,
- the decoupling between the instantaneous and delayed terms of the CTE,
- more sophisticated tests with complex histories of temperature,
- the influence of mineral additions (e.g. slag and fly ash), admixtures (e.g. superabsorbent polymer and superplasticizer) and the porosity of the aggregate at very early age on the development of the autogenous strain and the CTE,
- the influence of external drying during the hardening process on the development of the CTE and the autogenous strain.

References

Alungbe, G. D., Tia, M., & Bloomquist, D. G. (1992). Effects of aggregate, water/cement ratio, and curing on the coefficient of linear thermal expansion of concrete. *Transportation Research Record (TRR), 1335,* 44–51.

ASTM C403. (2008). Standard test method for time of setting of concrete mixtures by penetration resistance. *American Society of Testing and Materials*. https://doi.org/10.1520/c0403_c0403m-08.

ASTM C531-00. (2012). Standard test method for linear shrinkage and coefficient of thermal expansion of chemical-resistant mortars, monolithic surfacings and polymer concretes. *ASTM International*. 10.1520/C0531-00R12.Copyright.

ASTM Standard C1698. (2014). Test method for autogenous strain of cement paste and mortar. i(Reapproved 2014) (pp. 1–8). https://doi.org/10.1520/c1698-09r14.

Bangham, D. H., & Fakhoury, N. (1931). CLXXV.—The translation motion of molecules in the adsorbed phase on solids. *Journal of the Chemical Society*, 1324–1333. https://doi.org/10.1039/jr9310001324.

Barcelo, L., et al. (1999). Linear vs. volumetric autogenous shrinkage measurement: material behaviour or experimental artefact. In *Self-desiccation and its importance in concrete technology* (pp. 109–125). Available at: http://scholar.google.com/scholar?hl=en&q=Linear+vs.+volumetric+autogenous+shrinkage+measurements:+material+behaviour+or+experimental+artefact&btnG=&as_sdt=1,22&as_sdtp=#0.

Baroghel-Bouny, V. (1994). *Caractérisation des pâtes de ciment et des bétons, Méthodes, Analyse, Interprétation*. Ph.D. thesis, Ecole Nationale des Ponts et Chaussées.

Baroghel-Bouny, V., et al. (2006). Autogenous deformations of cement pastes. *Cement and Concrete Research, 36*(1), 123–136. https://doi.org/10.1016/j.cemconres.2004.10.020.

Bažant, Z. P. (1970). Delayed thermal dilatations of cement paste and concrete due to mass transport. *Nuclear Engineering and Design, 14*(2), 308–318. https://doi.org/10.1016/0029-5493(70)90108-1.

Bažant, Z. P. (1972). Thermodynamics of hindered adsorption and its implications for hardened cement paste and concrete. *Cement and Concrete Research, 2*(1), 1–16. https://doi.org/10.1016/0008-8846(72)90019-1.

Beltzung, F., & Wittmann, F. H. (2005). Role of disjoining pressure in cement based materials. *Cement and Concrete Research, 35*(12), 2364–2370. https://doi.org/10.1016/j.cemconres.2005.04.004.

Benboudjema, F., et al. (2019). Mechanical properties. In E. M. R. Fairbairn & M. Azenha (Eds.), *Thermal cracking of massive concrete structures—State of the art report of the RILEM Technical Committee 254-CMS* (pp. 69–114). https://doi.org/10.1007/978-3-319-76617-1_4.

Bentz, D. P. (2007). Transient plane source measurements of the thermal properties of hydrating cement pastes. *Materials and Structures, 40*(10), 1073–1080. https://doi.org/10.1617/s11527-006-9206-9.

Bentz, D. P., Garboczi, E. J., & Quenard, D. (1998). Modelling drying shrinkage in reconstructed porous materials: application to porous Vycor glass. *Modelling and Simulation in Materials Science and Engineering, 6*(1998), 211–236. https://doi.org/10.1088/0965-0393/6/3/002.

Bjontegaard, O. (1999) *Thermal dilation and autogenous deformation as driving forces to self-induced stresses in high-performance concrete*.

Bjøntegaard, Ø. (2011) *Basis for and practical approaches to stress calculations and crack risk estimation in hardening concrete structures—State of the art*.

Bjøntegaard, Ø., et al. (2015). *RILEM Technical Committee 195-DTD Recommendation for Test Methods for AD and TD of Early Age Concrete*. Dordrecht: Springer Netherlands (RILEM State-of-the-Art Reports). https://doi.org/10.1007/978-94-017-9266-0.

Bjøntegaard, Ø., Hammer, T., & Sellevold, E. J. (2004). On the measurement of free deformation of early age cement paste and concrete. *Cement & Concrete Composites, 26*(5), 427–435. https://doi.org/10.1016/S0958-9465(03)00065-9.

Bjøntegård, Ø., & Sellevold, E. J. (2001). Interaction between thermal dilation and autogenous deformation in high performance concrete. *Materials and Structures, 34*(239), 266–272. https://doi.org/10.1617/13731.

Bouasker, M. (2007). *Etude Numerique Et Experimentale Du Retrait Endogene Au Tres Jeune Age Des Pates De Ciment Avec Et Sans Inclusions*. Ph.D. thesis, Université de Nantes.

Bouasker, M., et al. (2008). Chemical shrinkage of cement pastes and mortars at very early age: Effect of limestone filler and granular inclusions. *Cement & Concrete Composites, 30*(1), 13–22. https://doi.org/10.1016/j.cemconcomp.2007.06.004.

Boulay, C. (2003) Determination of the coefficient of thermal expansion. In A. Bentur (Ed.), *Early age cracking in cementitious systems—Report of RILEM Technical Committee 181-EAS—Early age shrinkage induced stresses and cracking in cementitious systems* (pp. 217–224). RILEM Publications SARL.

Boulay, C., et al. (2010). Quasi-adiabatic calorimetry for concretes : Influential factors. *Bulletin des Laboratoires des Ponts et Chauss ees*, 19–36. Available at: https://hal.archives-ouvertes.fr/hal-00562100%5Cn.

Boulay, C. (2012). Test rig for early age measurements of the autogenous shrinkage of a concrete. In *Proceedings of the RILEM-JCJ International Workshop ConCrack 3* (pp. 111–122).

Boulay, C., et al. (2014). How to monitor the modulus of elasticity of concrete, automatically since the earliest age? *Materials and Structures, 47*(1–2), 141–155. https://doi.org/10.1617/s11527-013-0051-3.

Briffaut, M., et al. (2012). Effects of early-age thermal behaviour on damage risks in massive concrete structures. *European Journal of Environmental and Civil Engineering, 16*(5), 589–605. https://doi.org/10.1080/19648189.2012.668016.

Brooks, J., & Megat Johari, M. (2001). Effect of metakaolin on creep and shrinkage of concrete. *Cement & Concrete Composites, 23*(6), 495–502. https://doi.org/10.1016/S0958-9465(00)00095-0.

Cagnon, H., et al. (2016). Effects of water and temperature variations on deformation of limestone aggregates, cement paste, mortar and High Performance Concrete (HPC). *Cement & Concrete Composites, 71,* 131–143. https://doi.org/10.1016/j.cemconcomp.2016.05.013.

Campbell-Allen, D., & Thorne, C. P. (1963). The thermal conductivity of concrete. *Magazine of Concrete Research, 15*(43), 39–48. https://doi.org/10.1680/macr.1963.15.43.39.

Carette, J., & Staquet, S. (2015). Monitoring the setting process of mortars by ultrasonic P and S-wave transmission velocity measurement. *Construction and Building Materials, 94,* 196–208. https://doi.org/10.1016/j.conbuildmat.2015.06.054.

Charron, J. P. (2003). *Contribution à l'étude du comportement au jeune âge des matériaux cimentaires en conditions des déformations libre et restreinte*. Ph.D. thesis, Université Laval.

Chaunsali, P., & Mondal, P. (2016). Physico-chemical interaction between mineral admixtures and OPC–calcium sulfoaluminate (CSA) cements and its influence on early-age expansion. *Cement and Concrete Research, 80,* 10–20. https://doi.org/10.1016/j.cemconres.2015.11.003.

Coussy, O. (2003). The equivalent pore pressure and the swelling and shrinkage of cement-based materials. *Materials and Structures, 37*(265), 15–20. https://doi.org/10.1617/14080.

Craeye, B., et al. (2010). Effect of mineral filler type on autogenous shrinkage of self-compacting concrete. *Cement and Concrete Research, 40*(6), 908–913. https://doi.org/10.1016/j.cemconres.2010.01.014.

Cusson, D., & Hoogeveen, T. (2006). Measuring early-age coefficient of thermal expansion in high-performance concrete. In *International Rilem Conference* (pp. 321–330). https://doi.org/10.1617/2351580052.034.

Cusson, D., & Hoogeveen, T. (2007). An experimental approach for the analysis of early-age behaviour of high-performance concrete structures under restrained shrinkage. *Cement and Concrete Research, 37*(2), 200–209. https://doi.org/10.1016/j.cemconres.2006.11.005.

Darquennes, A. (2009). *Comportement au jeune âge de bétons formulés à base de ciment au laitier de haut fourneau en condition de déformations libre et restreinte*. Ph.D. thesis, Université Libre de Bruxelles.

Darquennes, A., Staquet, S., & Espion, B. (2011). Determination of time-zero and its effect on autogenous deformation evolution. *European Journal of Environmental and Civil Engineering, 15*(7), 1017–1029. https://doi.org/10.1080/19648189.2011.9695290.

Day, R. L. (1974). *Thermal deformation of cement paste*. Canada: The university of Calgari.

De Schutter, G., & Taerwe, L. (1995). Specific heat and thermal diffusivity of hardening concrete. *Magazine of Concrete Research, 47*(172), 203–208. https://doi.org/10.1680/macr.1995.47.172.203.

Delsaute, B. (2016). *New approach for monitoring and modelling of the creep and shrinkage behaviour of cement pastes, mortars and concretes since setting time*. Université Libre de Bruxelles (BATir) and Université Paris Est (IFSTTAR).

Delsaute, B., Boulay, C., & Staquet, S. (2016). Creep testing of concrete since setting time by means of permanent and repeated minute-long loadings. *Cement & Concrete Composites, 73,* 75–88. https://doi.org/10.1016/j.cemconcomp.2016.07.005.

Delsaute, Brice, & Staquet, S. (2017a). Decoupling thermal and autogenous strain of concretes with different water/cement ratios during the hardening process. *Advances in Civil Engineering Materials, 6*(2), 22. https://doi.org/10.1520/ACEM20160063.

Delsaute, B., & Staquet, S. (2017b). Impact of recycled aggregate in concrete on the evolution of the free deformation. In S. Staquet & D. G. Aggelis (Eds.), *Proceedings of the Second International RILEM/COST Conference on Early Age Cracking and Serviceability in Cement-based Materials and Structures*, Brussel (pp. 197–202).

Delsaute, B., & Staquet, S. (2018a). Impact de la présence de granulats et de sables recyclés sur le développement des propriétés du béton depuis la prise. In *NoMaD 2018* (p. 8).

Delsaute, B., & Staquet, S. (2018b). Influence of recycled aggregate and recycled sand on the development of the early age properties of concrete since setting. In *SynerCrete'18 International Conference on Interdisciplinary Approaches for Cement-based Materials and Structural Concrete* (pp. 231–236).

Delsaute, B., & Staquet, S. (2019). Development of strain-induced stresses in early age concrete composed of recycled gravel or sand. *Journal of Advanced Concrete Technology, 17*(6), 319–334. https://doi.org/10.3151/jact.17.319.

Delsaute, B., & Staquet, S. (2020). Impact of recycled sand and gravels in concrete on volume change. *Construction and Building Materials, 232* (under rev).

Emanuel, J. H., & Hulsey, J. L. (1977). Prediction of the thermal coefficient of expansion of concrete. *ACI Journal Proceedings, 74*(4), 149–155.

Eppers, S., & Mueller, C. (2008). Autogenous shrinkage and time-zero of UHPC determined with the shrinkage cone. In *8th International Conference on Creep, Shrinkage and Durability Mechanics of Concrete and Concrete Structures* (pp. 709–714). https://doi.org/10.1201/9780203882955.ch94.

Esping, O. (2008). Effect of limestone filler BET(H2O)-area on the fresh and hardened properties of self-compacting concrete. *Cement and Concrete Research, 38*(7), 938–944. https://doi.org/10.1016/j.cemconres.2008.03.010.

Feldman, R. F., & Sereda, P. J. (1968). A model for hydrated Portland cement paste as deduced from sorption-length change and mechanical properties. *Matériaux et Constructions, 1*(6), 509–520. https://doi.org/10.1007/BF02473639.

Ferraris, C. F., & Wittmann, F. H. (1987). Shrinkage mechanisms of hardened cement paste. *Cement and Concrete Research, 17*(3), 453–464. https://doi.org/10.1016/0008-8846(87)90009-3.

fib. (2013). *Code-type models for structural behaviour of concrete: Background of the constitutive relations and material models in the fib Model Code for Concrete Structures 2010*, *fib Bulletin 70*.

Fritsch, F., & Carlson, R. (1980). Monotone piecewise cubic interpolation. *SIAM J. Numer. Anal., 17*(2), 238–246. https://doi.org/10.1137/0717021.

Garcia Boivin, S. (1999). *Retrait au jeune âge du béton. Développement d'une méthode expérimentale et contribution à l'analyse physique du retrait endogène*. Ph.d. Thesis, ENPC/LCPC.

Grasley, Z. C., & Lange, D. (2006). Thermal dilation and internal relative humidity of hardened cement paste. *Materials and Structures, 40*(3), 311–317. https://doi.org/10.1617/s11527-006-9108-x.

Gutsch, A.-W. (2000). *Stoffeigenschaften jungen Betons – Versuche und Modelle*.

Hammer, T. A. (2003). Measurement methods for testing of early age autogenous strain. In *Early age cracking in cementitious systems—Report of RILEM Technical Committee 181-EAS—Early age shrinkage induced stresses and cracking in cementitious systems* (pp. 207–215).

Hammer, T. A., Bjøntegaard, Ø. (2006). Testing of autogenous deformation (AD) and thermal dilation (TD) of early age mortar and concrete—recommended test procedure. In *International RILEM Conference on Volume Changes of Hardening Concrete: Testing and Mitigation* (pp. 341–346). RILEM Publications. https://doi.org/10.1617/2351580052.036.

Hammer, T. A., Bjøntegaard, Ø., & Sellevold, E. J. (2003). Measurement methods for testing of early age autogenous strain. In: *Early age cracking in cementitious systems—Report of RILEM Technical Committee 181-EAS—Early age shrinkage induced stresses and cracking in cementitious systems* (pp. 217–228).

Hansen, W. (2011). Report on early-age cracking. *Concrete International, 33*(3), 2–5.

Instruments, T. (2017). *Tam air isothermal calorimetry*. Available at: http://www.tainstruments.com/pdf/brochure/TAM-AIR-brochure.pdf. Accessed February 14, 2017.

Jensen, O. M., & Hansen, P. F. (1999). Influence of temperature on autogenous deformation and relative humidity change in hardening cement paste. *Cement and Concrete Research, 29*(4), 567–575. https://doi.org/10.1016/S0008-8846(99)00021-6.

Jensen, O. M., & Hansen, P. F. (2001). Autogenous deformation and RH-change in perspective. *Cement and Concrete Research, 31*(12), 1859–1865. https://doi.org/10.1016/S0008-8846(01)00501-4.

Johnson, W. H., & Parsons, W. H. (1944). Thermal expansion of concrete aggregate materials. *Journal of Research of the National Bureau of Standards, 32*(3), 101–126. https://doi.org/10.6028/jres.032.002.

Kada, H., et al. (2002). Determination of the coefficient of thermal expansion of high performance concrete from initial setting. *Materials and Structures, 35*(245), 35–41. https://doi.org/10.1617/13684.

Koenders, E. A. B. (1997). *Simulation of volume changes in hardening cement-based materials*. Delft. Available at: http://repository.tudelft.nl/view/ir/uuid:1dbcb7fb-3f8f-466b-8517-b2235ad4912f/.

Kohno, K., et al. (1999). Effects of artificial lightweight aggregate on autogenous shrinkage of concrete. *Cement and Concrete Research, 29*(4), 611–614. https://doi.org/10.1016/S0008-8846(98)00202-6.

Königsberger, M., Delsaute, B., & Staquet, S. (2018). Evolution of thermal expansion coefficients during hydration of cement paste: Insights from experimental monitoring and thermo-poro-micromechanical modeling. In *ICEM18*, Brussels.

Kovler, K. (1994). Testing system for determining the mechanical behaviour of early age concrete under restrained and free uniaxial shrinkage. *Materials and Structures, 27*(6), 324–330. https://doi.org/10.1007/BF02473424.

Kronlöf, A., Leivo, M., & Sipari, P. (1995). Experimental study on the basic phenomena of shrinkage and cracking of fresh mortar. *Cement and Concrete Research, 25*(8), 1747–1754. https://doi.org/10.1016/0008-8846(95)00170-0.

Kumar Mehta, P., & Monteiro, P. J. M. (2006). *Concrete: Microstructure, properties, and materials* (4th ed.). Third. The McGraw-Hill Companies.

Laplante, P., & Boulay, C. (1994). Evolution du coefficient de dilatation thermique du béton en fonction de sa maturité aux tout premiers âges. *Materials and Structures, 27*(10), 596–605. https://doi.org/10.1007/BF02473129.

Le Chatelier, H. (1900). Sur le changement de volume qui accompagne le durcissement des ciments. *Bulletin de la Société de l'encouragement pour l'industrie nationale, 5*(5), 54–57.

Le Roy, R. (1995). *Déformations instantanées et différées des bétons à hautes performances*. Ph.D. thesis, Ecole Nationale des Ponts et Chaussées, Paris, France.

Liu, Z., & Hansen, W. (2016). Aggregate and slag cement effects on autogenous shrinkage in cementitious materials. *Construction and Building Materials, 121,* 429–436. https://doi.org/10.1016/j.conbuildmat.2016.06.012.

Lokhorst, S. J. (1998). *Deformational behaviour of concrete influenced by hydration related changes of the microstructure*.

Loser, R., Münch, B., & Lura, P. (2010). A volumetric technique for measuring the coefficient of thermal expansion of hardening cement paste and mortar. *Cement and Concrete Research, 40*(7), 1138–1147. https://doi.org/10.1016/j.cemconres.2010.03.021.

Loukili, A., et al. (2000). A new approach to determine autogenous shrinkage of mortar at an early age considering temperature history. *Cement and Concrete Research, 30*(6), 915–922. https://doi.org/10.1016/S0008-8846(00)00241-6.

Lura, P., & Durand, F. (2006). Volume changes of hardening concrete : testing and mitigation. In O. M. Jensen, P. Lura, & K. Kovler (Eds.), *Concrete* (pp. 57–65). Lyngby.

Maruyama, I., & Teramoto, A. (2011). Impact of time-dependant thermal expansion coefficient on the early-age volume changes in cement pastes. *Cement and Concrete Research, 41*(4), 380–391. https://doi.org/10.1016/j.cemconres.2011.01.003.

Maruyama, I., & Teramoto, A. (2012). Effect of water-retaining lightweight aggregate on the reduction of thermal expansion coefficient in mortar subject to temperature histories. *Cement and Concrete Composites, 34*(10), 1124–1129. https://doi.org/10.1016/j.cemconcomp.2012.08.003.

Maruyama, I., Teramoto, A., & Igarashi, G. (2014). Strain and thermal expansion coefficients of various cement pastes during hydration at early ages. *Materials and Structures, 47*(1–2), 27–37. https://doi.org/10.1617/s11527-013-0042-4.

Mehta, P. K. (1973). Mechanism of expansion associated with ettringite formation. *Cement and Concrete Research, 3*(1), 1–6. https://doi.org/10.1016/0008-8846(73)90056-2.

Mejlhede Jensen, O., & Freiesleben Hansen, P. (1995). A dilatometer for measuring autogenous deformation in hardening portland cement paste. *Materials and Structures, 28*(7), 406–409. https://doi.org/10.1007/BF02473076.

Min, D., & Mingshu, T. (1994). Formation and expansion of ettringite crystals. *Cement and Concrete Research, 24*(1), 119–126. https://doi.org/10.1016/0008-8846(94)90092-2.

Mindess, S., Young, J. F., & Darwin, D. (2003). *Concrete*. Upper Saddle River, NJ, USA: Prentice Hall, Pearson Education, Inc.

Milenkovic, N., et al. (no date). Advanced characterisation of the early age behaviour of bulk hydrophobic mortars. *Construction and Building Materials*.

Mitani, H. (2003). *Variations volumiques des matrices cimentaires aux très jeunes âges : approche expérimentale des aspects physiques et microstructuraux*. Ph.D. thesis, Ecole Nationale des Ponts et Chaussées.

Mitchell, L. (1953). Thermal expansion tests on aggregates, neat cements, and concretes. *Proceedings—American Society for Testing and Materials*.

Mohamed, M. S., et al. (2017). Applicability of ultrasonic measurement on the monitoring of the setting of cement pastes: effect of water content and mineral additions. *Advances in Civil Engineering Materials, 6*(2). https://doi.org/10.1520/acem20160062.

Mounanga, P., Khelidj, A., & Bastian, G. (2004). Experimental study and modelling approaches for the thermal conductivity evolution of hydrating cement paste. *Advances in Cement Research, 16*(3), 95–103. https://doi.org/10.1680/adcr.2004.16.3.95.

Nilsson, L. (1987). Temperature effects in RH measurements on concrete—some preliminary studies. In *Symposium and day of building physics* (pp. 456–462). Lund, Sweden: Swedish Council for Building Research.

Odler, I., & Colán-Subauste, J. (1999). Investigations on cement expansion associated with ettringite formation. *Cement and Concrete Research, 29*(5), 731–735. https://doi.org/10.1016/S0008-8846(99)00048-4.

Ozawa, M., & Morimoto, H. (2006). Estimation method for thermal expansion coefficient of concrete at early ages. In *International RILEM Conference on Volume Changes of Hardening Concrete: Testing and Mitigation* (pp. 331–3390. https://doi.org/10.1617/2351580052.035.

Paillere, A. M., & Serrano, J. J. (1976). Appareil d'étude de la fissuration du béton. *Bulletin de liaison du Laboratoire Central des Ponts et Chaussées, 83,* 29–38.

Persson, B. (2002). Self-desiccation and chloride migration. In *The Third International Research Seminar in Lund* (pp. 175–194).

Powers, T. C. (1965). Mechanisms of shrinkage and reversible creep of hardened cement paste. In *The structure of concrete and its behaviour under load*, London (pp. 319–344).

Powers, T. C. (1968). The thermodynamics of volume change and creep. *Materiaux et constructions, 1*(6), 487–507. https://doi.org/10.1007/BF02473638.

Radjy, F., Sellevold, E. J., & Hansen, K. K. (2003). Temperature data for water sorption in hardened cement paste: Enthalpy, entropy and sorption isotherms at different temperatures. In *Report R057* (p. 58). Available at: papers2://publication/uuid/345F4693-1D32-4D3D-A911-CA13EA5D47AA.

Roziere, E., et al. (2015). Experimental assessment of autogenous shrinkage. In *CONCREEP 2015: Mechanics and Physics of Creep, Shrinkage, and Durability of Concrete and Concrete Structures—Proceedings of the 10th International Conference on Mechanics and Physics of Creep, Shrinkage, and Durability of Concrete and Concrete Structure*. https://doi.org/10.1061/9780784479346.117.

Sant, G., Lura, P., & Weiss, J. (2006). A discussion of analysis approaches for determining "time-zero" from chemical shrinkage and autogenous strain measurements in cement paste. In *International RILEM Conference on Volume Changes of Hardening Concrete: Testing and Mitigation*, Lyngby (pp. 375–383). Available at: http://www.rilem.net/gene/main.php?base=500218&id_publication=57&id_papier=2271.

Sant, G., et al. (2011). The origin of early age expansions induced in cementitious materials containing shrinkage reducing admixtures. *Cement and Concrete Research, 41*(3), 218–229. https://doi.org/10.1016/j.cemconres.2010.12.004.

Scherer, G. W. (2000). Measuring permeability of rigid materials by a beam-bending method: I, Theory. *Journal of the American Ceramic Society, 83*(9), 2231–2239.

Scherer, G. W. (2003). Characterization of saturated porous bodies. *Materials and Structures, 37*(265), 21–30. https://doi.org/10.1617/14079.

Sellevold, E. J., & Bjøntegaard, Ø. (2006). Coefficient of thermal expansion of cement paste and concrete: Mechanisms of moisture interaction. *Materials and Structures, 39*, 809–815. https://doi.org/10.1617/s11527-006-9086-z.

Siddiqui, M. S., & Fowler, D. W. (2014). Optimizing coefficient of thermal expansion of concrete and its importance on concrete structures. *Construction Materials and Structures*, 47–56. https://doi.org/10.3233/978-1-61499-466-4-47.

Siddiqui, M. S., & Fowler, D. W. (2015). Effect of internal water pressure on the measured coefficient of thermal expansion of concrete. *Journal of Materials in Civil Engineering, 27*(4), 04014151. https://doi.org/10.1061/(ASCE)MT.1943-5533.0001095.

Staquet, S., et al. (2005). *Expérimentation sur poutres préfléchies à talon BTHP*, Paris.

Staquet, S., et al. (2019). Mixture proportioning for crack avoidance. In *Thermal cracking of massive concrete structures—State of the Art Report of the RILEM Technical Committee 254-CMS* (pp. 115–151). https://doi.org/10.1007/978-3-319-76617-1_5.

Stefan, L. (2009). *Étude Expérimentale Et Modélisation De L'Évolution Des Propriétés Mécaniques Au Jeune Âge Dans Les Matériaux Cimentaires*. Ecole normale supérieure de Cachan. Available at: http://tel.archives-ouvertes.fr/tel-00624989/.

Stefan, L., et al. (2018). Influential factors in volume change measurements for cementitious materials at early ages and in isothermal conditions. *Cement and Concrete Composites, 85,* 105–121. https://doi.org/10.1016/j.cemconcomp.2017.10.007.

Viviani, M., Glisic, B., & Smith, I. F. C. (2006). System for monitoring the evolution of the thermal expansion coefficient and autogenous deformation of hardening materials. *Smart Materials and Structures, 15*(6). https://doi.org/10.1088/0964-1726/15/6/n01.

Viviani, M., Glisic, B., & Smith, I. F. C. (2007). Separation of thermal and autogenous deformation at varying temperatures using optical fiber sensors. *Cement and Concrete Composites, 29*(6), 435–447. https://doi.org/10.1016/j.cemconcomp.2007.01.005.

Wang, H., et al. (2018). May reversible water uptake/release by hydrates explain the thermal expansion of cement paste?—Arguments from an inverse multiscale analysis. *Cement and Concrete Research*. https://doi.org/10.1016/j.cemconres.2018.05.008.

Wittmann, F. (1968). Surface tension, shrinkage, and strength of hardened cement paste. *Materiaux et constructions, 1*(6), 547–552. https://doi.org/10.1007/BF02473643.

Wittmann, F., & Lukas, J. (1974). Experimental study of thermal expansion of hardened cement paste. *Matériaux et Constructions, 7*(4), 247–252. https://doi.org/10.1007/BF02473853.

Wyrzykowski, M., & Lura, P. (2013a). Controlling the coefficient of thermal expansion of cementitious materials—A new application for superabsorbent polymers. *Cement and Concrete Composites, 35*(1), 49–58. https://doi.org/10.1016/j.cemconcomp.2012.08.010.

Wyrzykowski, M., & Lura, P. (2013b). Moisture dependence of thermal expansion in cement-based materials at early ages. *Cement and Concrete Research, 53,* 25–35. https://doi.org/10.1016/j.cemconres.2013.05.016.

Xi, Y., Bažant, Z. P., & Jennings, H. M. (1994). Moisture diffusion in cementitious materials Adsorption isotherms. *Advanced Cement Based Materials, 1*(6), 248–257. https://doi.org/10.1016/1065-7355(94)90033-7.

Yeon, J. H, Choi, S., & Won, M.C. (2009). Effect of relative humidity on coefficient of thermal expansion of hardened cement paste and concrete. *Transportation Research Record: Journal of the Transportation Research Board, 2113*(09), 83–91. https://doi.org/10.3141/2113-10.

Yeon, J. H., Choi, S., & Won, M. C. (2013). 'In situ measurement of coefficient of thermal expansion in hardening concrete and its effect on thermal stress development. *Construction and Building Materials, 38,* 306–315. https://doi.org/10.1016/j.conbuildmat.2012.07.111.

Zhutovsky, S., & Kovler, K. (2017). Application of ultrasonic pulse velocity for assessment of thermal expansion coefficient of concrete at early age. *Materials and Structures, 50*(1), 5. https://doi.org/10.1617/s11527-016-0866-9.

Ziegeldorf, S. W., Kleiser, K., & Hilsdorf, H. K. (1978). Effect of thermal expansion of aggregate on thermal expansion of concrete. Budapest. In *Colloque Internationale sur les materiaux granulaire/International symposium on aggregates and filler* (pp. 452–464).